INDUSTRIAL APPLICATIONS OF PRINCIPLES OF GREEN

CHEMISTRY

A Thesis
Presented to
The Academic Faculty

By

Swetha Sivaswamy

In Partial Fulfillment
Of the Requirements for
Master of Science (Thesis) in Chemical Engineering

Georgia Institute of Technology
August 2012

INDUSTRIAL APPLICATIONS OF PRINCIPLES OF GREEN CHEMISTRY

Approved by:

Dr. Charles A Eckert, Advisor
School of Chemical and Biomolecular Engineering
Georgia Institute of Technology

Dr. Charles L Liotta, Co-Advisor
School of Chemistry and Biochemistry
Georgia Institute of Technology

Dr. Amyn Teja
School of Chemical and Biomolecular Engineering
Georgia Institute of Technology

Date Approved: 3rd May 2012

ACKNOWLEDGEMENTS

For being my guiding light, Thank you God.

I would like to thank Professors, Dr Charles Eckert and Dr Charles Liotta, for giving me the opportunity to be a part of their outstanding research group for the past four years. Dr. Eckert's bottom line approach to executing projects is an invaluable learning for research and engineering. Dr. Liotta's enthusiasm for science is infectious and I have learnt a lot from interactions with him. My special thanks to Dr. Pamela Pollet for her attention to detail both with my experiments in the lab and the communication of results, and for the mentoring provided. I would like to recognize Dr Amyn Teja for serving on my committee.

Many past and present group members - Vittoria Blasucci, Emily Nixon, Kyle Flack, Amy Rohan, Jackson Switzer, Dr Manish Talreja, and Dr Rani Jha - have worked with me on the experiments over the past several years and whose contributions are present in this thesis. I would like to thank Dr. Gelbaum for the training provided on the NMR machines and for being an intellectual resource for both projects that I was a part of. Kevin Guger, from ChBE IT support, has been very helpful with any computer-related issues that I have had.

I also appreciate the CO_2 capture and avoidance group and the upstream corrosion testing group at ConocoPhillips, Bartlesville for the technical assistance in their labs over the summer of 2011. The internship opportunity provided by ConocoPhillips is also acknowledged.

Graduate school has been a bumpy road and even corridor conversations with people in the EST building and in our wing went a long way. Particularly, I wish to

TABLE OF CONTENTS

LIST OF TABLES

LIST OF FIGURES

SUMMARY

Cross-linked polyethylene has higher upper use temperature than normal polyethylene and is used as an insulating material for electricity carrying cables and hot water pipes. The most common method of inducing crosslinks is by reaction with silanes. After incorporation of silanes into polyethylene and upon hydrolysis with ambient moisture or with hot water, Si-O-Si crosslinks are formed between the various linear polyethylene chains. Industrially, this reaction is performed routinely. However, the efficiency of this reaction with respect to the silane is low and control of product distribution is difficult. The grafting reactions were studied in the laboratory using hydrocarbon models of polymers – heptane, dodecane. The primary goal of the project was to gain a precise fundamental understanding so that we would be able to manipulate the reactions and thus, allow for the facile processing of the polymers. Chapter 1 discusses the grafting reactions and the advanced NMR techniques that we have conducted towards this goal.

Scalable and cost effective methods to capture CO_2 are important to counterbalance some of the global impact of the combustion of fossil fuels on climate change. Amines, especially monoethanolamine, have been the most commercialized technology. However, it is not without disadvantages. House et al have investigated the energy penalty involved in the post-combustion CO_2 capture and storage from coal-fired power plants and found that 15-20% reduction in the overall electricity usage is necessary to offset the penalty from capturing and storing 80% of United States coal fleet's CO_2 emssions[1]. Novel non-aqueous amine solvents, developed by the Eckert Liotta group, react with CO_2 to form ionic liquids. The ionic liquids readily desorb CO_2 upon heating, regenerating the reactive

amines and this cycle can be carried out multiple times. An iterative procedure is being adopted to develop amine solvents for CO_2 capture using structure/property relationships and is dealt with in Chapter 2. On reaction with CO_2, there is a sharp increase in viscosity which is unfavorable from a processing standpoint. Many approaches to mitigate and control viscosity will be discussed.

[1]*House et al, Energy Environ Sci, 2009, 2, 193-205*

.

CHAPTER 1

FUNDAMENTAL STUDIES ON RADICAL INITIATED SILANE GRAFTING OF POLYETHYLENE USING HYDROCARBON MODELS

Introduction

The process of incorporating silanes in polyethylene is an important reaction to induce cross-links in polyethylene[1]. Controlled crosslinking in polymers provides for enhanced physical properties, such as heat resistance, impact strength and chemical resistance, without impairing other essential characteristics like ease of processing and high tensile strength[2]. A review paper by Morshedian[3] et al gives a comprehensive list of changes of properties of polyethylene after crosslinking. These crosslinked polyethylene's (PE) have widespread uses as foams for insulation material and in the cable jacketing industry. Ordinary PE is unsuitable for applications requiring continuous use under stresses at temperatures up to 100°C. With a drastic improvement in properties after crosslinking, these materials have been used even for heat resistant food packaging up to 200°C [4].

The industrial process of crosslinking, known as the two-step Sioplas method, involves the reactive extrusion of a mixture of polyethylene and silane in the presence of peroxide[3]. The grafted polymer is pelletized and stored in sealed vacuum bags. Whenever required, the pellets are exposed to steam in the presence of a catalyst and cross-links are induced. Ease of processing, low cost and capital investment, and favorable properties of the final product are the advantages of silane crosslinking technology[5]. However, organosilane compounds are expensive and reactions may be limited by mass transfer.

Since the future of the wiring, cabling and tubing markets in the world is related to silane crosslinking, more detailed information on this subject is important. Although there is extensive

literature available on grafting with polyolefins with various functional molecules, there is a lack of fundamental understanding to make the crosslinking process more efficient for industrial use. During the industrial Sioplas process, a large amount of the grafting agent silane remains unreacted. Peroxide is used for the initiation of the reaction and it results in a wide distribution of products and controlling the extent of grafting is difficult[6]. This work explores the mechanistic and the stereochemical aspects of the grafting of silane onto polymeric models, and it is expected that the knowledge can be extended to bigger hydrocarbons as well.

Background

There are multiple pathways in which a radical propagation reaction between a long chain hydrocarbon and vinyltrimethoxysilane (VTMS) can proceed (Figure). The peroxide radical abstracts hydrogen from the hydrocarbon, creating a reactive site on the backbone. The double bond of the VTMS then adds to the reactive side resulting in an alpha-silyl radical as shown in the figure below. The initially formed graft radical can propagate through three main pathways.

1. Oligomeric grafting: The first graft reacts further with another VTMS and results in a polymeric graft dangling off the dodecane backbone. The tendency for VTMS to homopolymerize does not occur in the presence of peroxide initiators, presumably for steric reasons, so this possibility is minimal[6].

2. Intermolecular hydrogen atom transfer: The radical abstracts hydrogen from another PE backbone resulting in isolated single grafts.

3. Intramolecular hydrogen atom transfer: The radical abstracts hydrogen from the same hydrocarbon chain resulting in multiple single grafts on the same hydrocarbon. This can

15

occur either as 1, 3 hydrogen shift or as 1, 4 hydrogen shift or as 1, 5 hydrogen shift.

Figure elucidates these shifts using a diagram.
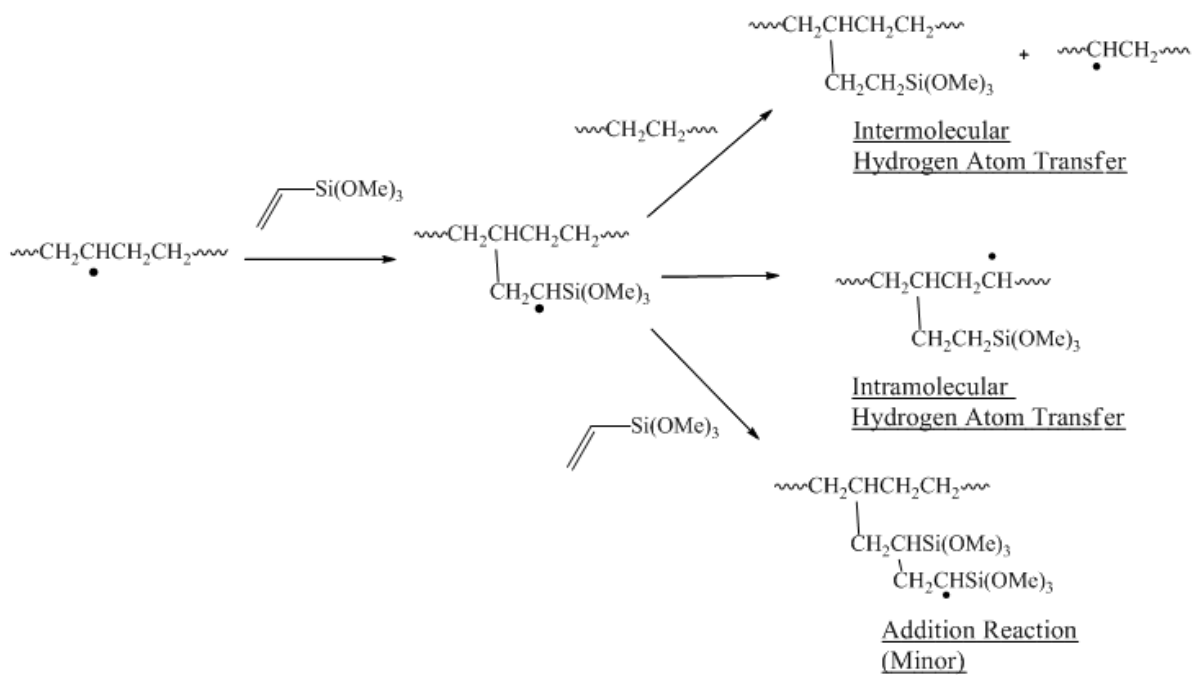
Figure : Major pathways of radical propagation
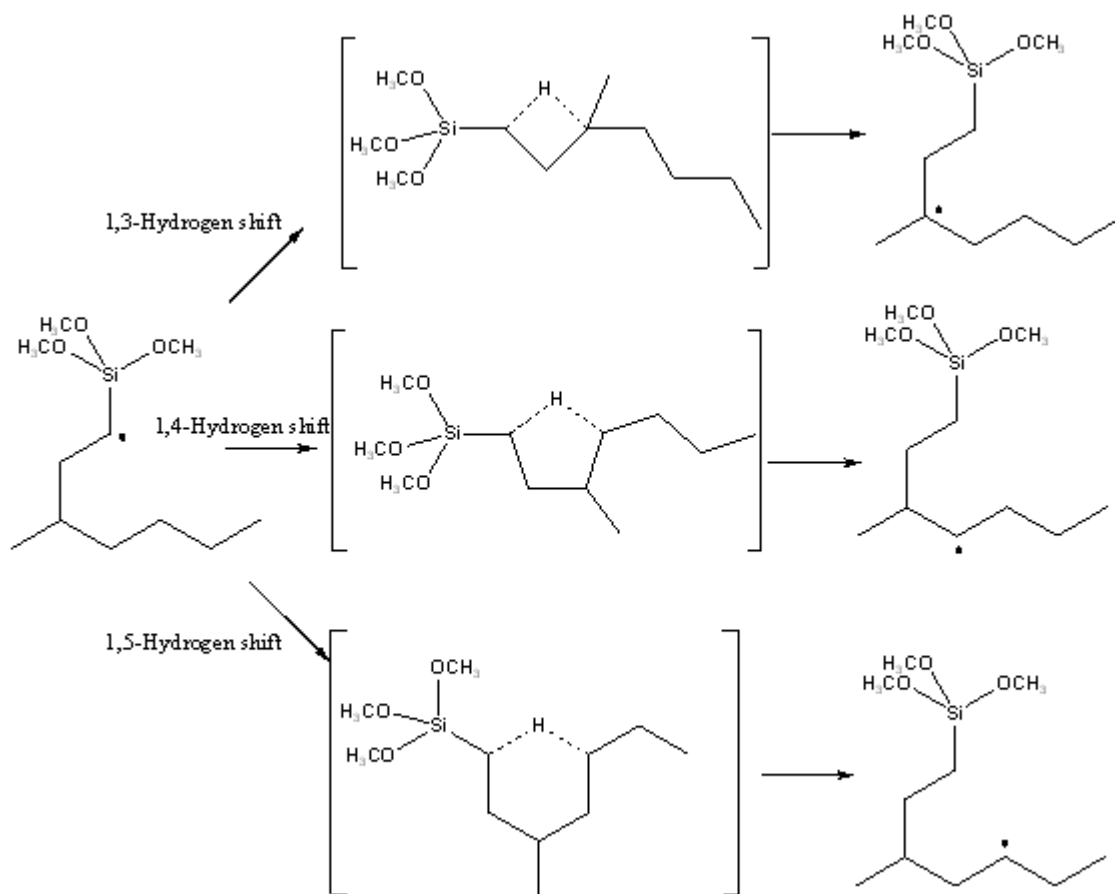
Figure : Intermolecular hydrogen transfer using 1,3 or 1,4 or 1,5 shift

Forsyth et al[6] have conducted related grafting studies with vinyltrimethoxysilane on dodecane as the model system, and the product mixture was found to be grafted with an average of 2.37 silane grafts per dodecane molecule and with around 59% conversion. Many analytical techniques were performed (FTIR, NMR, MS and GPC) which strongly indicated that the multiple grafts were predominantly multiple single grafts rather than homopolymer grafts. Also, they say that the grafts propagate through 1, 5 intermolecular hydrogen atom transfer although very little evidence is given in support of this hypothesis. We will discuss this aspect in detail along with our work in the latter part of this chapter.

17

Spencers's study[7] expanded upon this by the characterization of the VTMS-grafted-high density polyethylene and the structural analysis of model compounds. On separation and analysis of the grafted products of VTMS with tetradecane, they found high levels of multi-grafted products. They propose an alternate pathway for the intramolecular hydrogen transfer by which the free radical is transferred via a 1, 4 hydrogen shift.

The non-uniform distribution of grafted products on the polymer chain has been the motivation for a study by Weaver et al[8]. They use a silane functionalized nitroxyl (TEMPO) derivative for grafting and the product grafted with VTES consisted of only monografted species as against the average of 2.37 from Forsyth's work.

Towards this, we conducted a systematic investigation on model compounds representative of ethylenic polymers - dodecane and heptane - to provide insights on the mechanism of radical-initiated silane grafting, thus allowing for the development of efficient functionalization of ethylenic polymers. The reactions with model compounds were used to prepare various grafted compounds. Kinetic studies of the length of the quenching reaction with phenyllithium have led to interesting conclusions about the time required for complete substitution. Isolation and NMR studies on these fractions have led us to believe that 1, 4 hydrogen shift occurs along with the 1, 5 hydrogen shift. There has also been evidence leading to the suggestion that clusters of VTMS could exist in the hydrocarbon leading to multi-grafting. Also, compounds like CO_2, ethyltrimethoxysilane (ETMS) and tetramethoxyorthosilicate (TMOS) were added to reaction mixture to investigate the diluting effect on the clusters. This research is funded by DOW chemical company and we appreciate the continual interactions and feedback by their researchers - Jeffrey Cogen and Bharat Chaudhary - towards this work.

Experimental:

Materials:

All chemicals were sourced from Sigma Aldrich and used as received - dodecane (anhydrous, 99%), heptane (anhydrous, 99%), vinyltrimethoxysilane (98%), di-tert-butylperoxide (98%), ethyl acetate (CHROMASOLV®, for HPLC, ≥99.7%), phenyllithium (1.8M in di-n-butyl ether), tetrahydrofuran (CHROMASOLV® Plus, for HPLC, ≥95%), Hexane (CHROMASOLV® Plus, for HPLC, ≥95%). A solution of 0.3 mL of di-tert-butylperoxide in 10 mL of heptane was prepared and stored in the refrigerator to be used when required. CO_2 and N_2 are from Airgas cylinders with purity in excess of 99.9%.

Standard grafting reactions of VTMS with hydrocarbon models:

The experimental procedure was based on the work of Forsyth et al[6]. The grafting reactions were run with dodecane/heptane as a model for ethylenic polymers. vinyltrimethoxysilane (VTMS) was used as the grafting agent because of its prevalence in the industry. Prior to the reaction, the Parr® reactor was placed under vacuum. Heptane (50 mL), VTMS (5 wt %, 1.8 mL), di-tert-butylperoxide in heptane solution (1.1 mL of the solution, 750 ppm of peroxide in the reaction mixture), and either ethyltrimethoxysilane (5 wt %, 1.8 mL) or tetramethylorthosilicate (5 wt %, 1.7 mL) were added under 1 bar of N_2. After completion of the reaction, the reaction mixture was cooled to ambient temperature. Four equivalents of Phenyllithium (1.8 M in n-butylether) were added and stirred at room temperature for 24 hr as quoted in literature[6]. This was done to replace the reactive methoxy groups with unreactive phenyl groups for ease of analysis. There will be an extensive discussion on this time duration

19

later in this chapter. At the end of the quenching period, excess phenyllithium was quenched with a saturated solution of ammonium chloride. The organic and aqueous phase were separated and dried with magnesium sulfate. Prior to analysis, the sample was distilled using short path (at 80°C) and rotovapped to remove excess solvent. Samples were analyzed using matrix assisted laser desorption/ionization (MALDI) mass spectrometry with a dithranol matrix in combination with silver tetrafluoroacetate (AgTFa) to aid in ionization and by HPLC, ^{1}H and ^{13}C NMR.

Reactions with diluents – ETMS, TMOS, CO_2, N_2

For reactions with diluent compounds - ethyltrimethoxysilane (ETMS) and tetramethoxyorthosilicate (TMOS) - the above procedure was carried out in the same order. When adding reagents to the Parr autoclave for a reaction with ETMS, 5wt% of ETMS was added <u>in addition</u> to the compounds mentioned for the control reaction. The same holds true for TMOS reaction as well.

The reactions were also conducted under high pressures of nitrogen and carbon dioxide. After adding the reagents to the Parr, the desired gas (approximately 1/3rd of the required level of pressure) was added to the reaction mixture using a high pressure syringe pump (ISCO) at ambient temperature. The Parr was then heated to the reaction temperature (200°C) to account for the increase in pressure due to the evaporation of the reagent components. Pressure was then further added till it reached the desired value. This mixture reacted for 7 hours at 200°C, after which the gas was vented into flask containing tetrahydrofuran. The system was placed under vacuum before addition of phenyllithium, when CO_2 was used to ensure the elimination of any undesired side reactions. The rest of the experimental procedure was the same as above.

Kinetic studies for quenching time with phenyllithium:

For the kinetic studies of time of phenyllithium quenching, a Radleys Carousel 12 Station (Figure) was used. A series of twelve duplicate reactions with dodecane as the model were conducted under the same conditions; two reactions were quenched every day for a week. The reaction vessels in the carousels are smaller and the quantities of the reagents were scaled down to fit them. The station is equipped with argon lines and temperature control as well.

Figure : Radleys Carousel 12 Station

Separation of grafted fractions:

For the separation of the grafted product mixture (heptane-g-vinyltriphenylsilane), a centrifugal thin layer chromatography device known as chromatotron was used initially. 500 mg of the distilled mixture was added onto the prepared plate of silica gel and the solvent (95 hexane: 5 ethyl acetate) was used to elute the various components. However, due to low purity of separated fractions, a preparative normal phase HPLC was subsequently used according to Spencer et al[7]. Waters 2690 separations module (Supelcosil PLC-LC column, 25 cm by 21.2 mm,

5 μm particle size) with a UV-Vis detector and a solvent mixture of 99% hexane and 5% ethyl acetate was used. 70-200 μL of the product mixture was used for the injection and the peaks were collected as they appeared. Fractionation was insensitive to structural isomers. The collected fractions were sent for MALDI analysis for identification of the various compounds. Repeated injections provided enough material for NMR. The peaks were re-injected to ascertain purity of the sample.

Advanced NMR experiments:

^1H and ^{13}C NMR spectra were obtained using a Varian Mercury Vx 400 in $CDCl_3$. The 2D NMR experiments were carried out with a Bruker DRX-500 using an indirect detection probe. In order to keep the concentrations as high as possible, the samples were dissolved in 200 μL of solvent and placed in a solvent-matched Shigemi NMR tube. All experiments were run using standard Bruker pulse sequences, edited HSQC (hsqcedetgp)[9] and HSQC-TOCSY (hsqcetgpml).[10]

Dynamic light scattering:

The Stokes radii of the VTMS clusters were measured using dynamic light scattering (DLS). DLS experiments were performed by a single-mode optical fiber coupled to an avalanche photodiode detector using a Dynapro DLS (Wyatt Technology Corporation, Santa Barbara, CA). Because of the similarity of the refractive indices of hexane (refractive index n^{20}_D 1.387) and VTMS (refractive index n^{20}_D 1.392), the DLS experiments were conducted in dodecane (n^{20}_D 1.421) providing for higher contrast. Solutions of varying concentrations of VTMS - 5, 8, 10, 20, 30, 40, 50 percent weight of dodecane - were prepared in dodecane and used for the study of the

clusters. The correlation function data presented is an average of at least twenty measurements with acquisition times of 40 s.

Results and Discussion:

A standard reaction between dodecane and VTMS was carried out according to the experimental procedure described (Figure). The MALDI mass distribution of the final product mixture is as shown in Figure . The product distribution consists of 1-6 silane grafts on a single molecule of dodecane.
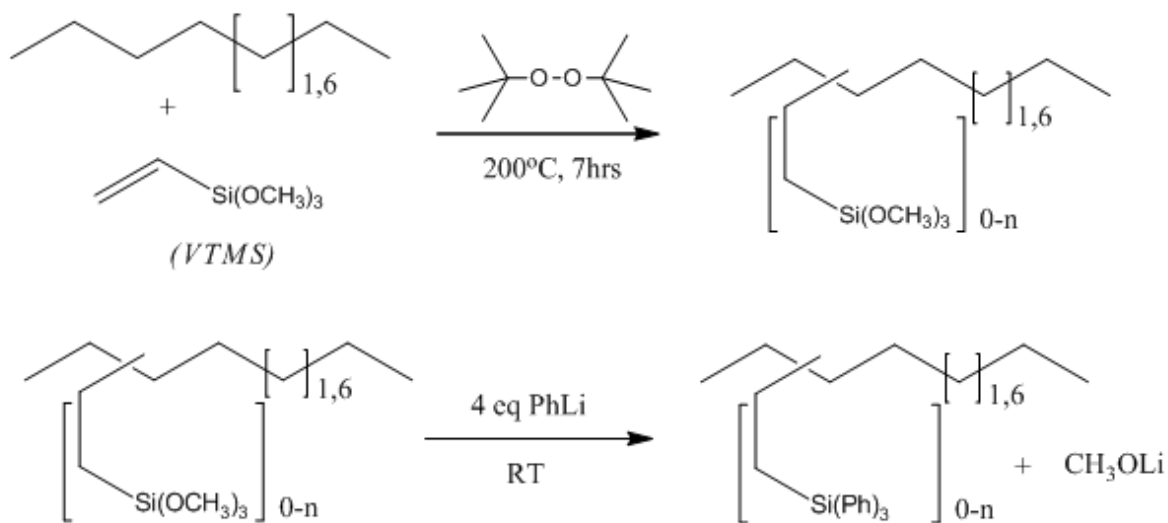
Figure : Step 1 - Reaction with VTMS; Step 2 - Quenching with Phenyllithium

On prolonged standing, a white solid crashed out of the above reaction product; this is believed to be the high molecular weight crosslinked material. In the case of complete substitution of all methoxy groups by phenyl groups, this would not have occured. ^{1}H NMR of the solid shows a small peak in the methoxy region (3.5 ppm), consistent with the incomplete quenching reaction as expected. MALDI MS analysis of the solid product showed up to 8 silane

grafts per dodecane, which was higher than the distribution obtained for the control reaction. Figure shows the skewed MALDI mass spectrum

This result is possibly due to the steric bulk of the phenyl groups. If one considers a dodecane molecule with a single silane graft, the quenching reaction results in the substitution of the three methoxy groups by phenyls, considerably increasing the steric bulkiness around the silane. Now if one considers a dodecane with 5 grafts, it is easier to understand that upon reaction with phenyl lithium the molecule quickly becomes sterically hindered—making it very hard to reach the methoxy groups for further reaction.
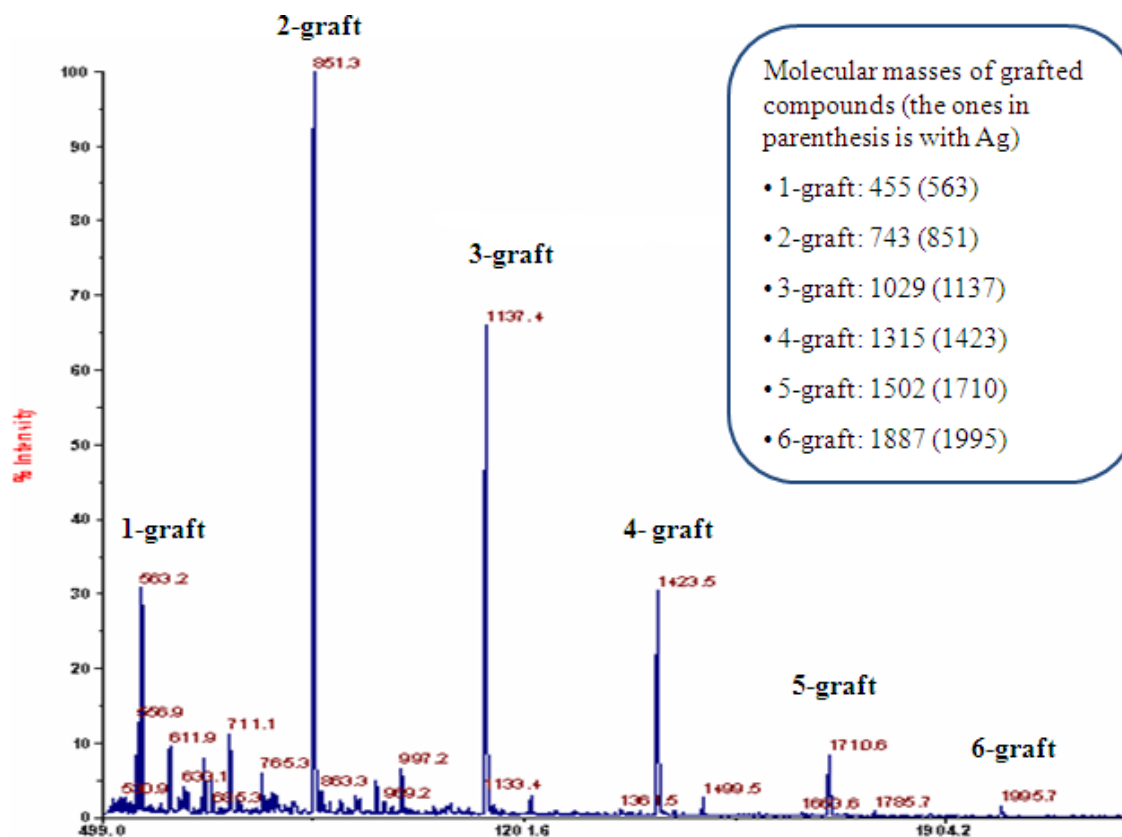
Figure : MALDI-MS of the grafted products from a dodecane reaction

The figure shows a MALDI-MS spectrum with labeled peaks. Peak groups are labeled 3-graft, 4-graft, 5-graft, 6-graft, 7-graft, and 8-graft. Various mass values are labeled including 999.3, 887.2, 1423.6, 1709.7, 851.3, 1137.4, 1135.4, 995.2, 921.2, 909.2, 901.3, 1151.4, 1283.4, 1707.7, 1995.8, 993.8, 2283.0, 2281.0, 2570.1, and others. A callout box reads:

> Molecular masses of grafted compounds (the ones in parenthesis is with Ag)
> • 1-graft: 455 (563)
> • 2-graft: 743 (851)
> • 3-graft: 1029 (1137)
> • 4-graft: 1315 (1423)
> • 5-graft: 1502 (1710)
> • 6-graft: 1887 (1995)
> • 7-graft: 2175 (2283)
> • 8-graft: 2462 (2570)

Note: mono- & di- grafts on a separate spectra

Figure : MALDI-MS of the solid crosslinked material

Two approaches were devised to circumvent the problem of incomplete substitution – longer quenching time and smaller quenching group. The latter was done by investigating a less sterically hindered organolithium salt like methyllithium. However, analysis of the product was complicated by the fact that the molecular weights were too low for MALDI –MS and complete fragmentation was seen when analyzed by other mass spec methods like fast atom bombardment. NMR experiments were not of much help because of the overlap between the peaks of the backbone and the methyl groups. Therefore, MeLi for quenching was not pursued further.

The reaction was then performed with an increased time for the phenyllithium quenching reaction. To determine the minimum time for complete substitution of the methoxy groups, we used a Radleys Carousel 12 Station to run a series of reaction. 12 duplicate reactions were conducted under the same conditions; two reactions were quenched everyday for a week. 1H

25

NMR of the product mixture was taken every day to monitor the disappearance of the methoxy peak. After Day 3, no white precipitate crashed out of the solution and the methoxy peaks from the ^{1}H NMR were insignificant (Figure). For our further studies, phenyllithium was continued to be used for quenching and the duration was increased from 24 hours to 72 hours to allow time for complete substitution. This was a significant finding because the time period quoted in the literature[6] would have not yielded the correct distribution of products.
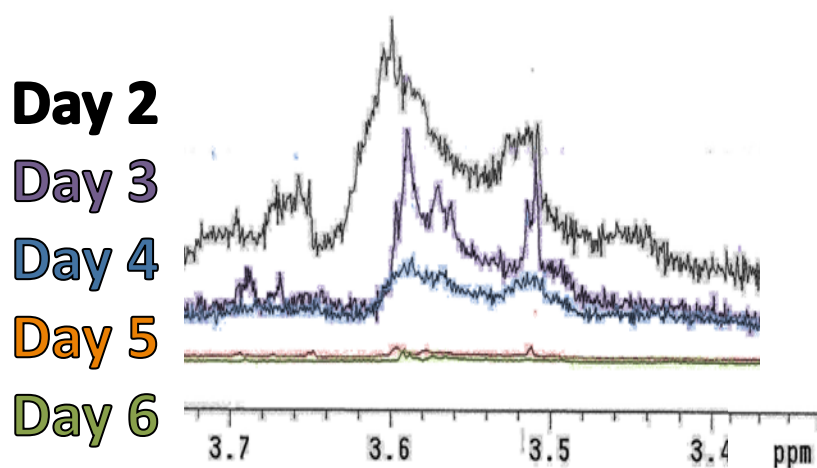
Figure : Overlay of NMR's depicting the disappearance of the methoxy peak

Later in the research, Lithiopyridine and 2-thienyllithium were also used in place of phenyllithium, for easier ionization and faster analysis. This could eliminate the preferential complexation of Ag to the grafted products. Lithiated-pyridine was prepared by stirring butyllithium and bromopyridine (1:1.2 mol ratio) in dry ether for three hours. The excess of bromopyridine was used to drive to reaction to completion. The resulting lithiated-pyridine and bromobutane mixture was added to the Parr after the reaction, instead of phenyllithium. Experiment was not a success because of the formation of butane (basic butyllithium abstracts a hydrogen from the acidic alpha-silyl product) in the Parr reactor leading to a pressure build-up

and was not performed again due to safety reasons. 2-thienyllithium was used as purchased for quenching instead of phenyllithium. But since the analysis did not yield pertinent results, this route was not pursued.

Heptane was used as a simpler hydrocarbon model for VTMS grafting and for the easier analysis of the products. On reaction with phenyllithium for three days and with analysis with MALDI, 1-5 silane grafts were seen on a single heptane molecule (Figure).
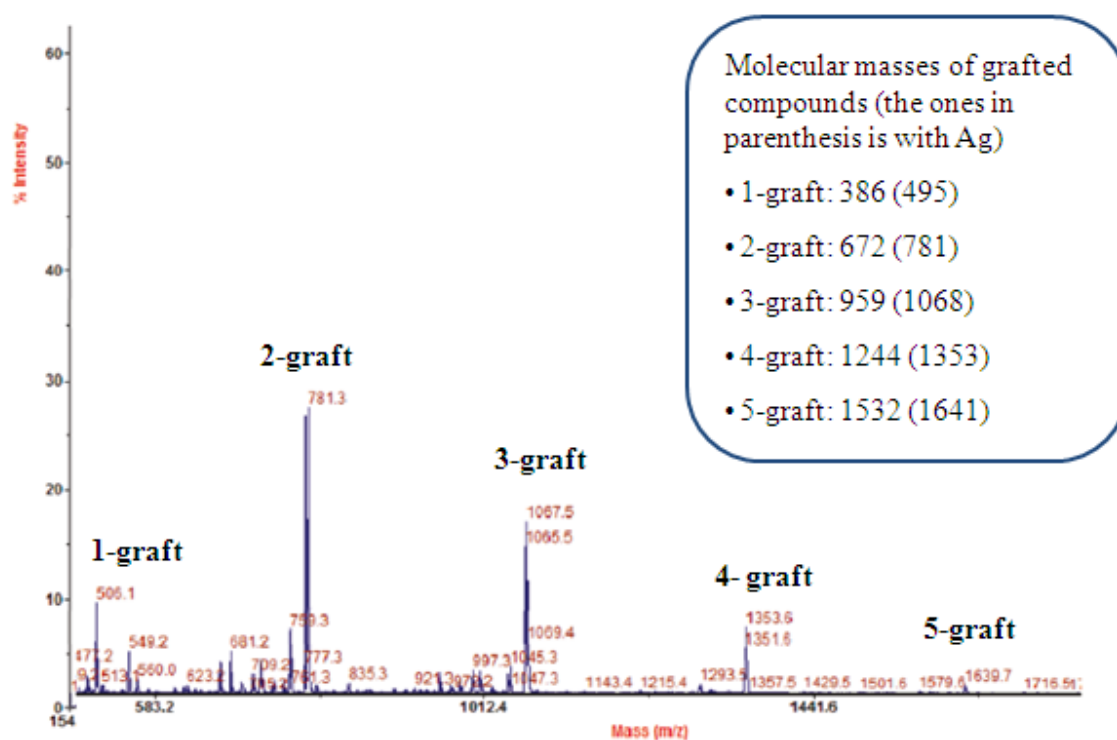
Figure : MALDI-MS of the reaction product from heptane

We have described earlier the occurrence of up to 8 silane grafts per dodecane. The increased amount of grafting could be due to oligomeric nature and to test this possibility, reactions were run in dodecane with different quantities of VTMS - 1 wt%, 10wt%, 50wt% - other than the standard 5 wt%. Table shows product distribution obtained on using the various

amounts of VTMS. Analysis via MALDI did not show an increase in the number of grafts. If oligomeric grafting were happening, the increased amount of grafting material should have resulted in increased grafting.

Table : Effect of the concentration of VTMS on grafting

VTMS (in wt %)	Number of grafts	Repeats
1	1 - 2	2
5	1 - 6	2
10	1 - 4	2
50	1 - 4	1*

The amount of phenyllithium required to quench the 50 wt% reaction was very high (>150 ml) and it was decided to not duplicate for safety reasons.

Although MALDI MS gives us information on the number of grafts on the dodecane chain, there is very little information on where exactly the grafting occurs. The first silane graft that attaches to the dodecane chain can happen on any carbon. For a two grafted dodecane, the second graft can be 1,2 or 1,3 or 1,4 etc. to the first silane graft and thus many permutations are possible. Many structural isomers exist with the complexity increasing exponentially for the higher grafted fractions. These structurally isomeric compounds do not show up differently in mass spectrometry and overlap in NMR's making it very difficult to distinguish them separately. For our research, advanced NMR techniques like DEPT NMR (Distortionless Enhancement by Polarization Transfer) and COSY (2-Dimensional correlation spectroscopy) were selected as possible methods to know the graft position. These NMR methods require highly pure (>99%) samples in order to prevent misinterpretation of the spectra and to pinpoint the regiochemistry

and possibly stereochemistry. Therefore, separations were carried out on a preparative scale HPLC even though it was known that they would be time-consuming.

Preparative HPLC was used directly in the crude sample of the heptane reaction. The HPLC spectrum consisted of multiple peaks of varying intensities. The grafted components elute in the order of increasing molecular weight. The exit stream corresponding to the peaks was timed and collected and analyzed using MALDI MS. Figure shows the HPLC spectrum along with the information gained from MALDI.

Apart from the regular 1-5 silane grafted heptane compounds, mono grafted di-heptane, vinyl triphenyl silane and triphenyl (2-phenylethyl) silane were obtained as side products. Subsequently, 2-g-heptane and 5-g-heptane were chosen to be isolated. Several runs of the HPLC were required to obtain material enough for NMR. The different structural isomers of the multiple grafted compounds did not appear as separate peaks on HPLC and were thus collected together.

Approximately, 10 mg of the 2-g-heptane was isolated and the purity was checked using NMR, MALDI and HPLC. A single peak at 781 on the mass spectrum and an isolated peak on the LC spectrum (Figure) ensured that the sample used for the advanced NMR studies were of purity >99%. Further, the ratio of aromatic to aliphatic protons on the 1H NMR spectrum of the isolated sample was 1.33 whereas the theoretical ratio was 1.36. 15 mg of the 5-g-heptane was also isolated and a single peak at 1639 on the mass spectrum and a single peak on the LC spectrum indicate high purity of the sample isolated (Figure).
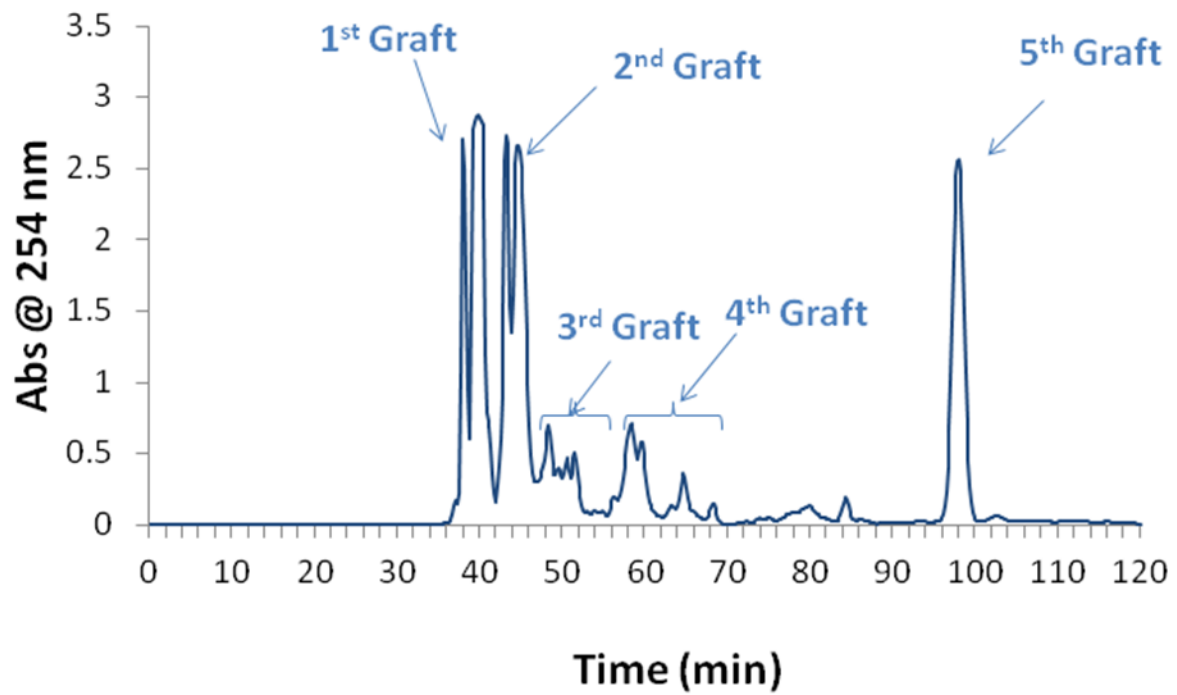
Figure : HPLC spectrum of the crude grafted product mixture
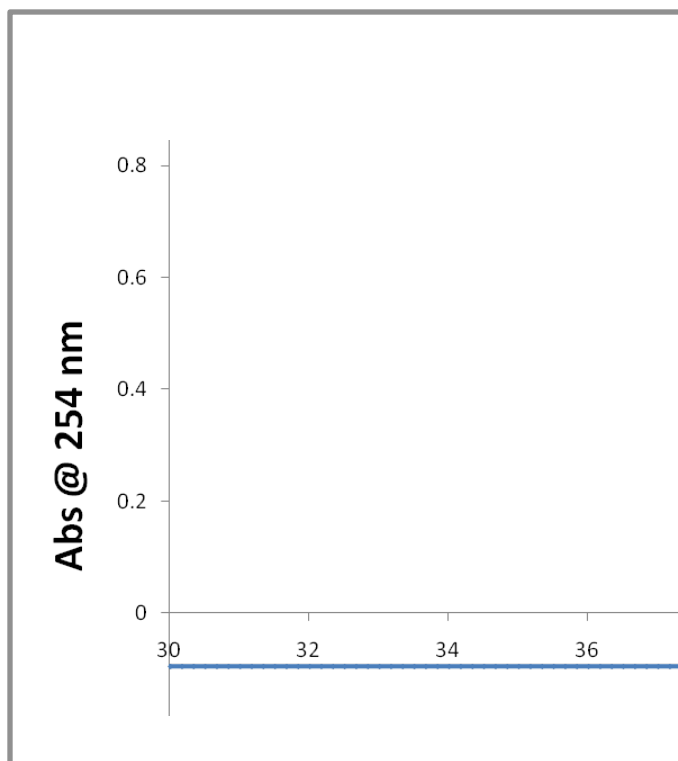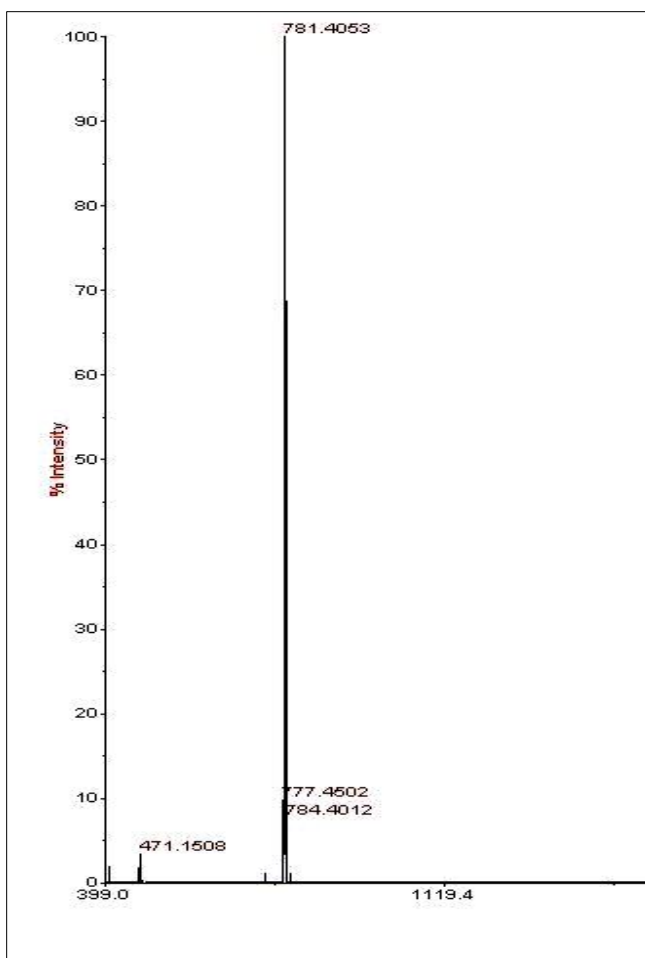
Figure : MALDI-MS and HPLC spectrum of isolated 2-g-heptane
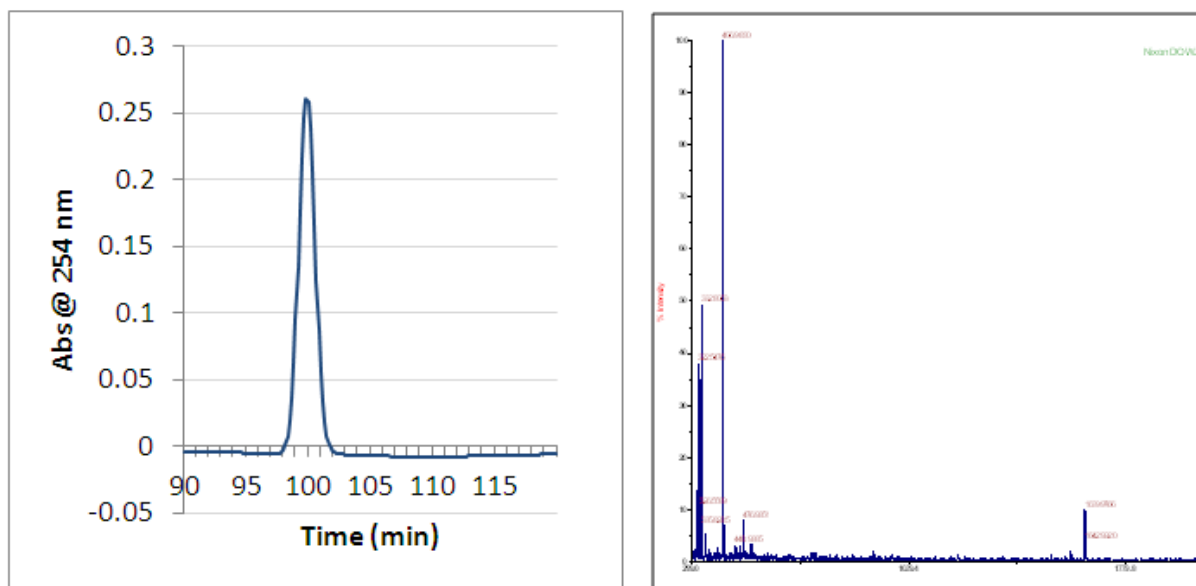
Figure : LC Spectrum and MALDI MS of the 5-g-heptane

The isolated grafted fractions were added along with 200 µL of CDCl₃ into the shigemi tube and sealed with paraffin paper. 2D NMR techniques – edited HSQC, HSQC-TOCSY – were performed on the samples to obtain information about the structural isomers and the regiochemistry of the samples. The edited HSQC correlated the ^{1}H NMR with the ^{13}C in a manner similar to the DEPT 135. The HSQC-TOCSY provides information about the groups adjacent to the chosen groups – a powerful tool to determine grafting position along the chain.

The intermolecular hydrogen shifts can indeed take place either by 1, 3 or 1, 4 or 1, 5 hydrogen shift as discussed earlier. Theoretically, the 1,3 hydrogen shift was found to be at least 10 kJ/mol less favorable than the 1,4 and 1,5 shift using transition state simulations via density functional theory (DFT, BYL3P-6.31G*). The possible products for the 2-grafted heptane formed by the initial formation of a radical at the 2-, 3-, 4- positions separately by 1,3 and 1,4 and 1,5 abstraction are shown in the Figure and Figure .

X = CH$_2$CH$_2$Si(Ph$_3$)
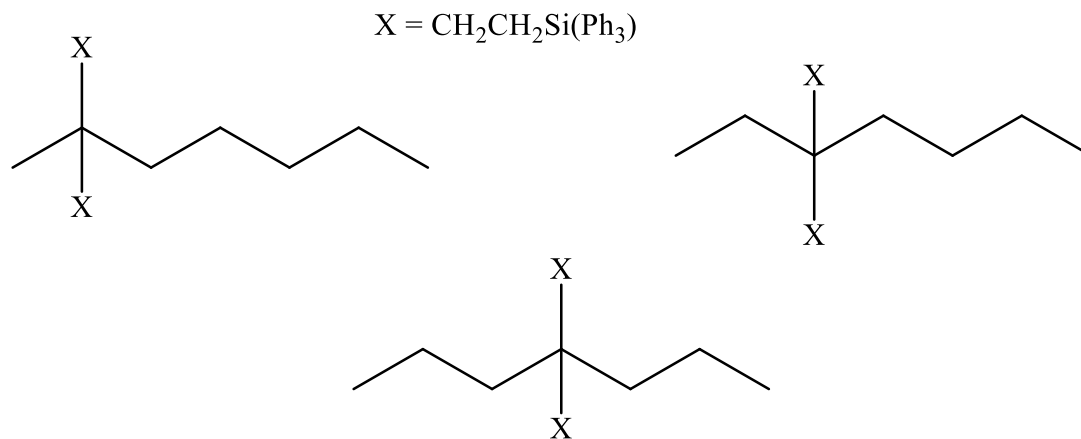
Figure : Possible structural isomers from 1,3 hydrogen shift

X = CH$_2$CH$_2$Si(Ph$_3$)
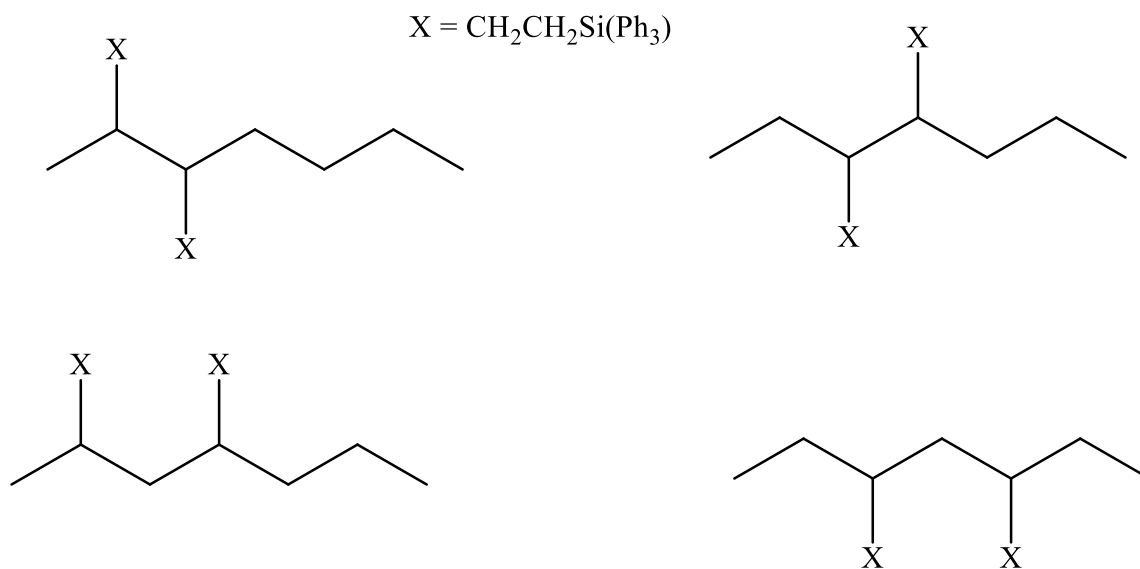
Figure : Possible structural isomers from 1, 4 and 1, 5 hydrogen shift

The combined ^{13}C, DEPT 135, and APT (Attached Proton Test) showed that no quaternary carbons were present; only CH, CH$_2$, and CH$_3$ signals were observed, ruling out the formation of products 1, 2, and 3. In the edited HSQC spectrum shown in Figure , the red signals represent CH$_2$'s while the signals in black represent CH's and CH$_3$'s. The six signals on the bottom left of the spectrum indicate the presence of six distinct CH groups. An HSQC-TOCSY experiment gives us additional information that two of those CH signals correlate with a

corresponding CH$_3$ signal (Figure) which signify that one of the grafts is present on the second carbon.
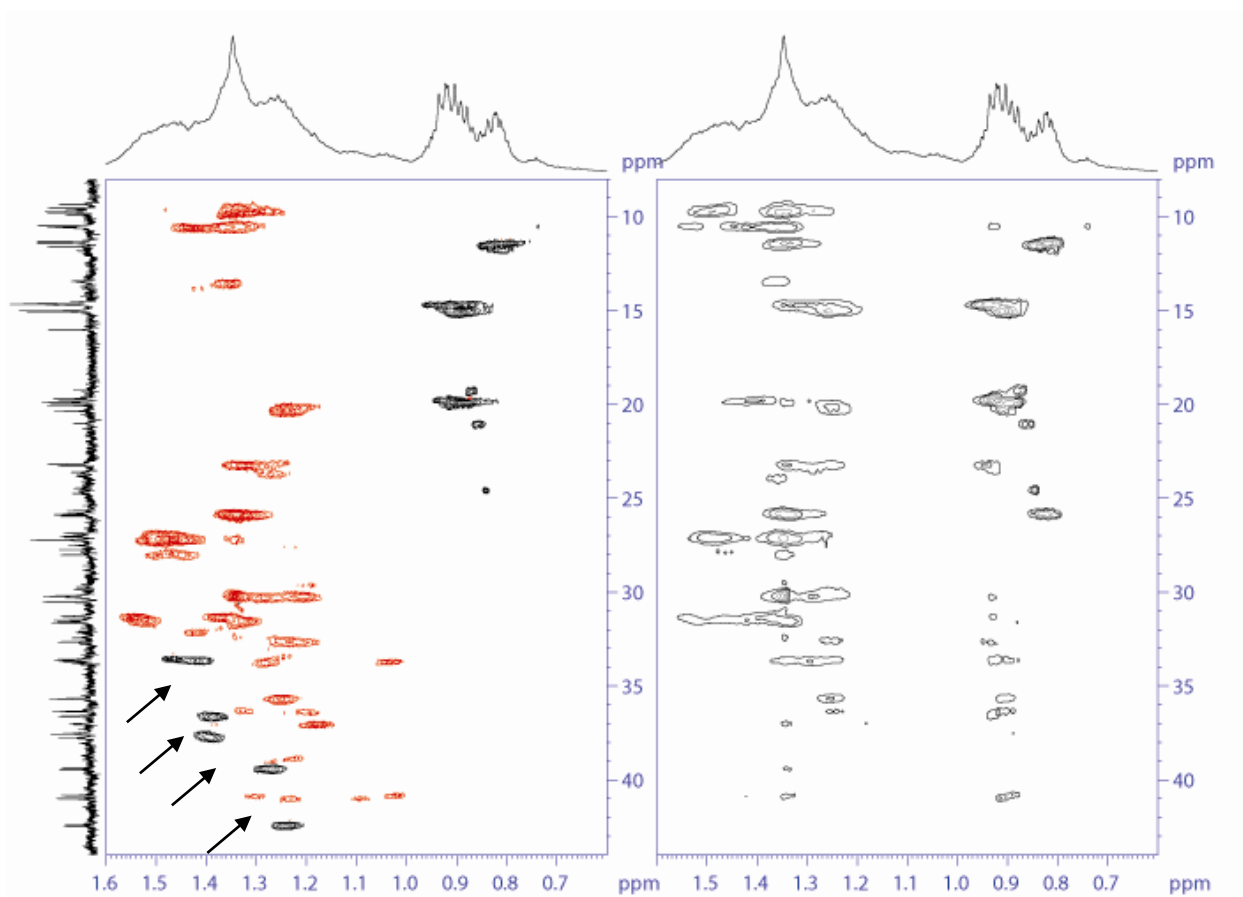
Figure : HSQC of 2-g-heptane
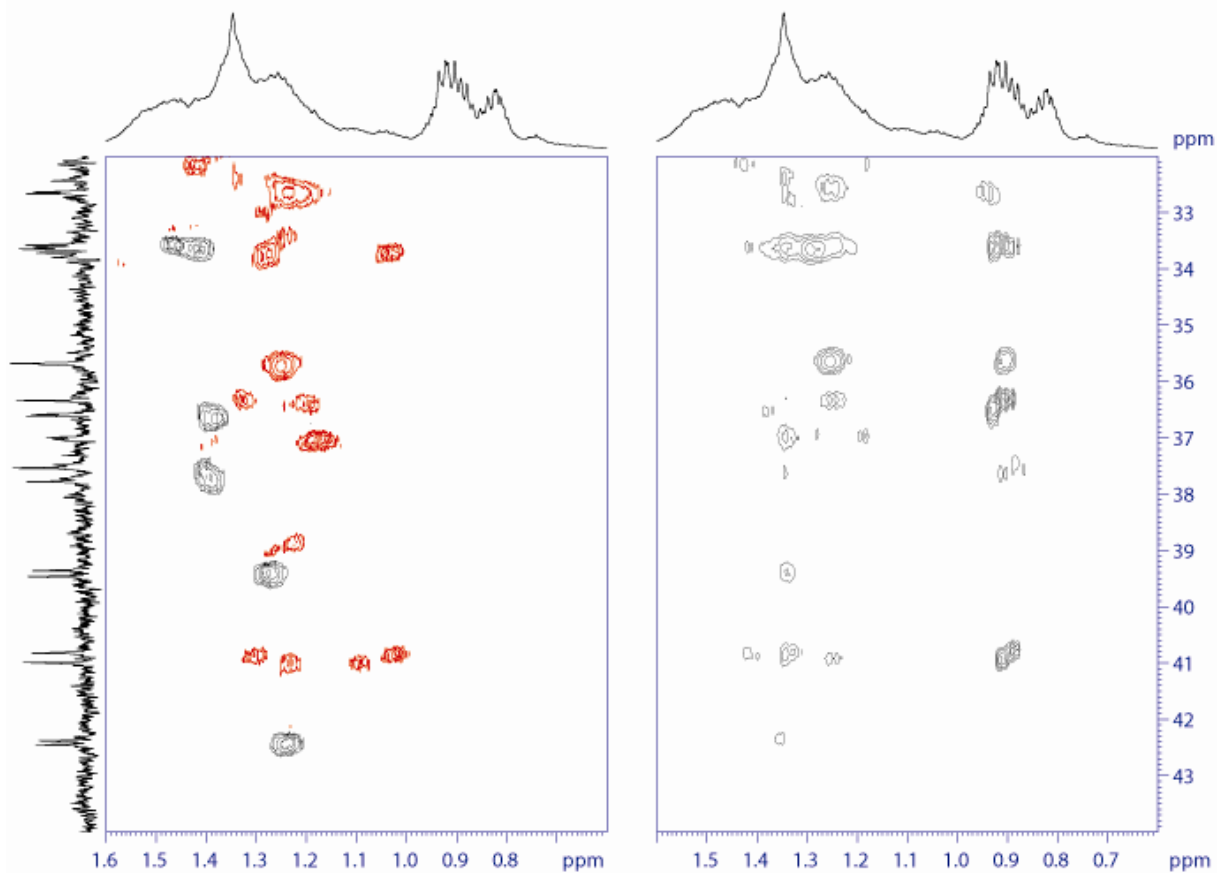
Figure : HSQC-TOCSY of 2-g-heptane

After elimination of the various possibilities from Figure and Figure using the conclusions from NMR, the following four structures remain (Figure). The assumptions include: 1) since multi-grafted heptanes are the major products from the analyses, intermolecular hydrogen abstraction is the most favorable pathway for the reaction to proceed. 2) Terminal grafting doesn't happen as it is energetically unfavorable to form a radical on a primary carbon[11].
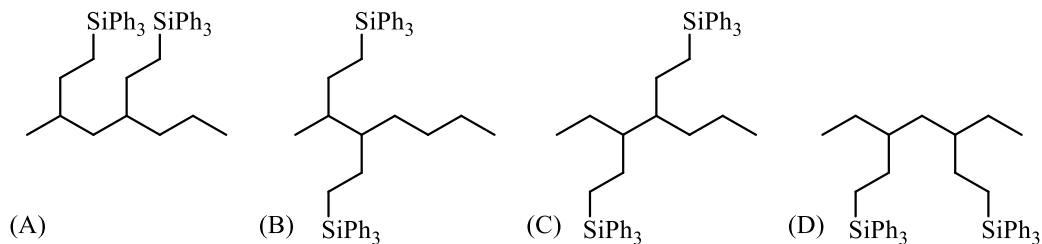
Figure : Structures of 2-g-heptane consistent with NMR

From the APT-DEPT experiment on the penta-grafted compound (Figure), a single quaternary carbon as detected indicates the possibility of two grafting events on the same carbon. The structures consistent with the NMR data, tell us that the radical propagation is most certainly not taking place with 1, 5 hydrogen shift alone.
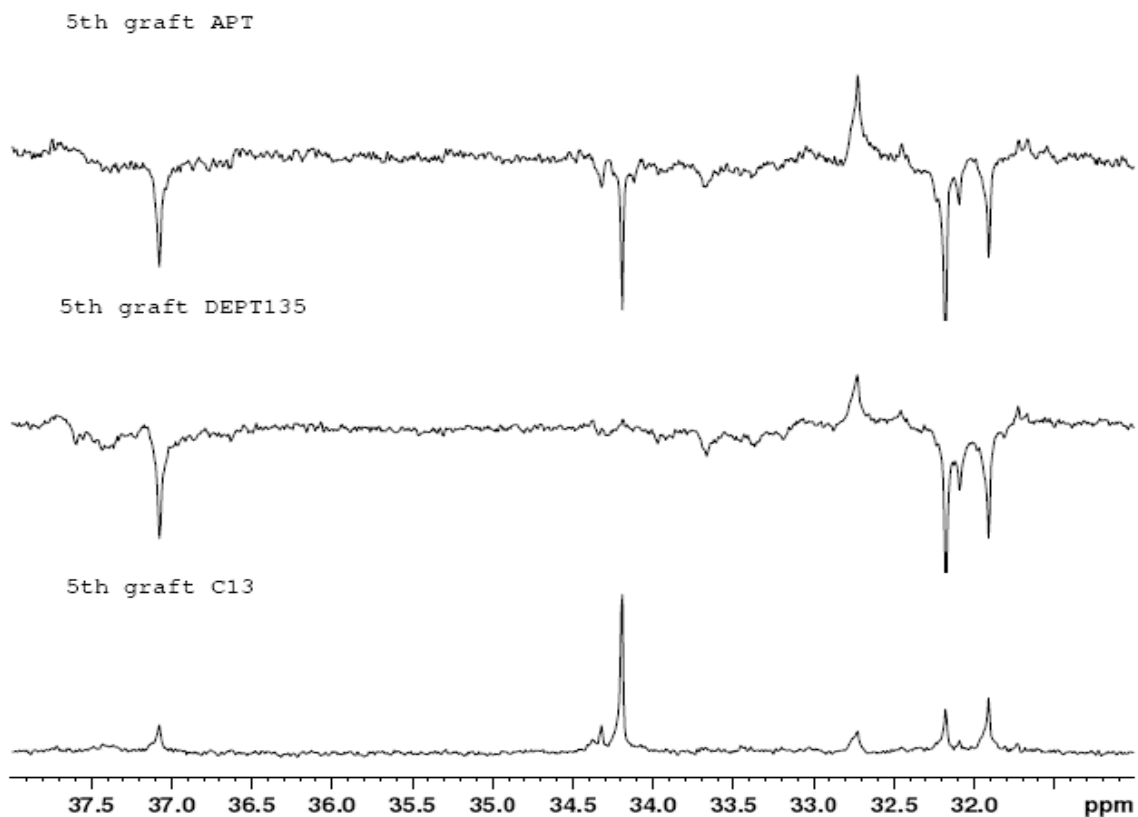
Figure : APT-DEPT of 5-g-heptane

The possibility of two simultaneous grafting events seems statistically improbable. Considering that the VTMS is added in such low concentrations and is the limiting reagent, it is easy to imagine the presence of few VTMS molecules in a sea of dodecane. If this were, indeed, the case, single grafting of the hydrocarbons is more likely than multiple grafting. A preliminary hypothesis is that VTMS forms clusters in the presence of dodecane. Multiple grafting would be highly probable if the local concentration of VTMS was higher adjacent to the initially-formed alpha-silyl radical. To test this hypothesis, Dynamic light scattering experiments were performed with pure dodecane and with 10 wt% VTMS in dodecane.

For dilute colloidal dispersions, dynamic light scattering is a popular method to determine the size of the particles. When a monochromatic beam of light, like laser, impinges on a solution of spherical particles it causes a shift and results in change of wavelength of incoming light. This change is related to the size of the particle and can be computed using simple equations.

The representative correlation functions from the experiments were compared and the smooth and continuous exponential decay curve for the solution of VTMS in dodecane is characteristic of cluster/particles in solution. As a control, the flat nature of the correlation function of pure dodecane implies that the absence of any clusters (Figure). The DLS experiments were performed on dodecane at room temperature. With the assumption that the clusters persists at 200°C, this suggests that the local concentration of VTMS near the radical site is enhanced and conducive to multi-grafting.
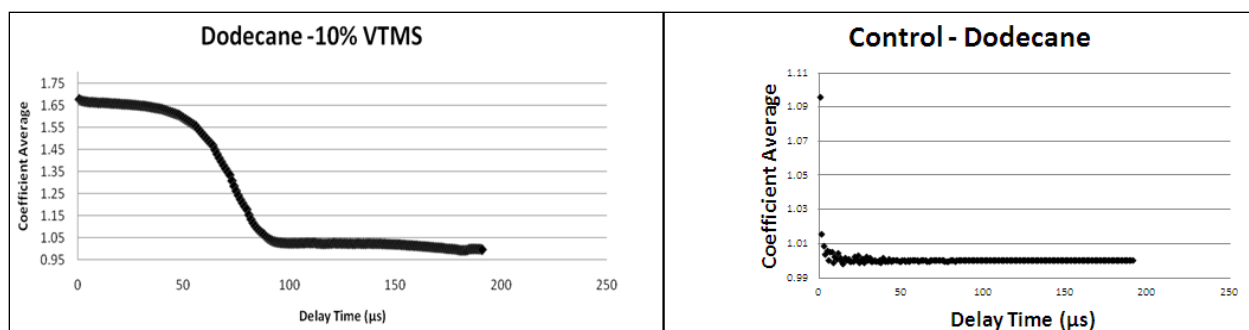
Figure : Representative correlation functions from DLS experiments

After confirming the presence of aggregates, dynamic light scattering experiments were conducted using varying amounts of VTMS in dodecane: 5 – 50 wt%. The nature of the correlation functions indicated the presence of aggregates at all concentrations of VTMS higher than 10 wt%. The average dynamic radius of VTMS clusters was determined to be 100 ± 20 nm for the concentrations 10-30 % wt. At higher concentration of 40 % and 50 % wt of VTMS we observe an increase in dynamic radii to 126 ± 4.40 and 189 ± 1.60 nm respectively which is a characteristic property of high concentrated solution resulting in the multiple scattering. There is a general upward trend of increase of size of particle to the increase in concentration of VTMS but they are not directly proportional. Although the instrument was not sensitive enough to measure clusters at 5 and 8 wt% (experimental conditions), perhaps the general inferences can be extrapolated to include that lower range as well. The number of molecules per cluster was calculated using stokes diameter with values of molar density and Avagadro's law (Table).

Table : Average stokes radius for different concentrations of VTMS in dodecane

VTMS in dodecane (wt %)	Avg. Stokes radius (nm)	Number of molecules per cluster
5	-	-
8	-	-
10	110 ± 4	2.19×10^7
20	114 ± 6	2.44×10^7
30	92 ± 9	1.28×10^7
40	126 ± 4	3.30×10^7
50	189 ± 2	1.11×10^8

One of the fundamental aims from an industry point of view, as said earlier, was to be able to control the distribution of grafting. The suggestion of clusters of VTMS is a step in the direction. We hypothesized that diluting the clusters would probably help control how the grafting proceeds. Three compounds were identified and tested – CO_2, ETMS and TMOS.

CO_2 was chosen because silane grafting of polyethylene is routinely performed at 2000-3000 psi in a reactive screw extruder in the industry and we wanted to investigate the use of CO_2 at these pressures. It is believed that CO_2 can help improve the solubility of the silanes in the molten polymer and help with uniform mixing.[12] Reactions were performed with dodecane and VTMS under three pressures of CO_2 – 1000 psi, 1500 psi, 2000 psi and with quenching with phenyllithium for one day only. Grafting distributions from MALDI indicate that the highest grafted product (6-g-dodecane) is not present in any of the products from the high pressure experiments. To determine whether hydrostatic pressure alone is contributing to the changes in the grafting distribution, the experiments were repeated with similar pressures of nitrogen.

Further, the MALDI peak intensities of all the high pressure experiments were plotted after normalizing it with respect to the intensity of the second graft (Figure). For experiments at 1000 psi, 6-g-dodecane was found in the case of N_2 but not in the case of CO_2. 6-g-dodecane and 5-g-dodecane were absent for 1500 CO_2; while the products were identical for 2000 psi N_2 and CO_2. Also, it has to be kept in mind that the accuracy of the MALDI distributions at lower molecular weights (1-g-dodecane, 2-g-dodecane) is lesser than at higher molecular weights. It is hard to tell whether the higher pressures of either gas results in a significant change of the grafting distributions as MALDI is, at best, semi-quantitative.

ETMS and TMOS would be two chemical molecules that would participate in the clustering (similar to the chemical structure of VTMS) but not in grafting. Both of these compounds lack the vinyl group which is the reactive site in radical-initiated grafting, and therefore will be unable to graft onto a hydrocarbon backbone by the standard radical addition process. Our typical reaction conditions use 5 wt % of VTMS; we added an equivalent wt % of the diluent molecule, anticipating that half of the clusters would then comprise of VTMS and the other half of diluent. Experiments were conducted on heptane as the model compound. The product mixtures, by MALDI analysis, showed the same product distribution as the control without the diluents compounds viz. 1-6 g heptane. Thus, qualitatively, comparable grafting patterns were obtained with or without the diluents (CO_2, ETMS, and TMOS). More quantitative analysis needs to be performed to obtain a clearer picture into the products.
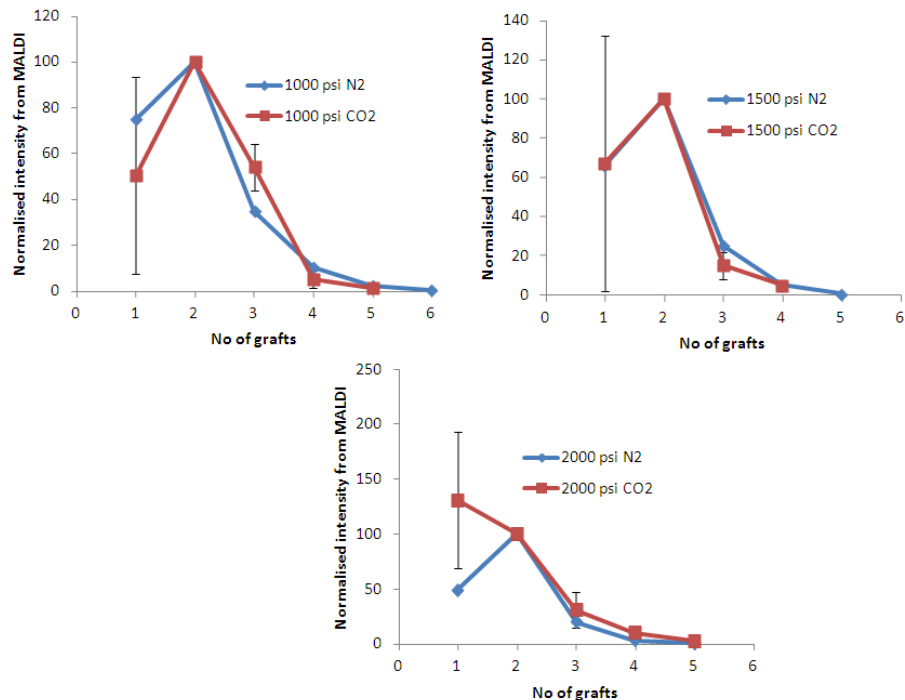
Figure : Variation in the intensity of the grafted portions (with respect to the second graft) for three pressure of CO₂
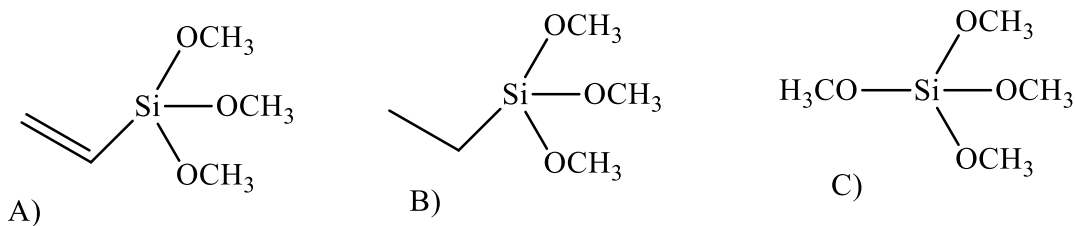
Figure : Structures of ETMS (B), TMOS (C) and VTMS (A)

However, the DLS results were more interesting. Previous results with dodecane and 10 wt% VTMS indicated an S-shaped curve suggestive of clusters. A similar trend was seen with 5 wt% VTMS – 5wt% ETMS solution as well (Figure) indicating that ETMS was participating the clusters. If they were not, the curve would be flat as like the case of 5 wt% VTMS – 5 wt% TMOS. This is because having aggregates from only a 5wt% VTMS solution would have been

too low for the detector limit of the DLS instrument used. The similarity of the chemical structures of ETMS and VTMS explains the fact that they participate in clustering.

With all three diluent molecules used – CO_2, ETMS, TMOS – the change in the distribution of grafts were not significant from MALDI. A more quantitative method of analysis of products will provide us a better picture into the product distribution.

Conclusions

A fundamental understanding of the grafting reactions was gained about the grafting reaction of VTMS on polyethylene. A greater time was required for the phenyllithium quenching reaction – for 72 hours instead of the 24 hours -- a significant finding as a shorter time would result in an incorrect distribution of the actual products formed during the grafting reaction.

Advanced NMR studies have resulted in data consistent with the 1, 4 and 1, 5 hydrogen shift as competing pathways for the radical propagation. There is conclusive evidence for the presence of one quaternary carbon in the penta-graft.

We are still continuing to investigate the big picture as to why multi-grafted products are the predominant pathway by which the reaction proceeds. DLS experiments support the hypothesis of formation of aggregates of VTMS in dodecane unequivocally from 10 wt% to 50 wt% VTMS. Qualitative MALDI produces the same distribution for reactions with and without the diluents – CO_2, ETMS, TMOS - compounds.

Path forward and recommendations

The model compounds that have been used in this work have different probabilities of forming a radical (primary, secondary, tertiary etc.) and thus, to eliminate this factor out of the regiochemistry and mechanism studies, I suggest the use of a model compound like cyclooctane (Figure) with equivalent carbons. There is preliminary literature on use of cyclooctane[8] as the model compound and our experiments have pointed out to the existence of 1-6 silane grafted compounds using MALDI. Isolation of the grafted compounds, especially the 2-grafted cyclooctane, and performing NMR studies similar to what has been done here would add a significant dimension to this work.
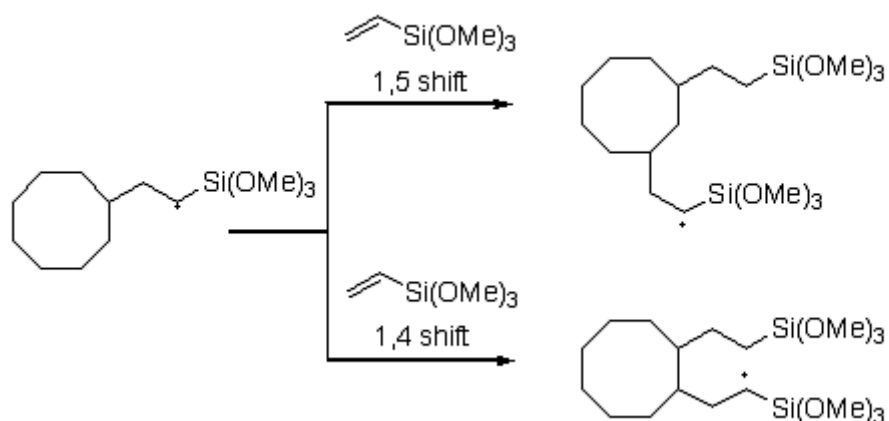
Figure : Possible products with grafting reactions with cyclooctane

References:

1.   Hjertberg, T.; Palmlof, M.; BA, S., Chemical reactions in cross-linking of copolymers of ethylene and vinyltrimethoxysilane. *Journal of applied polymer science* 1991, 42, 1185-1192.

2.   Pollet, P.; Liotta, C.; Charles, E.; Verma, M.; Nixon, E.; Sivaswamy, S.; Jha, R.; Momin, F.; Gelbaum, L.; Chaudhary, B. I.; Cogen, J. M., Radical mediated graft modification of polyolefin models with vinyltrimoethoxysilane: A fundamental study. *Industrial and Engineering Chemistry Research* 2011, (50), 12246-12253.

3.   Barzin, J.; Azizi, H.; Morshedian, J., Preparation of Silane-Grafted and Moisture Crosslinked Low Density Polyethylene. Part II: Electrical, Thermal and Mechanical Properties. *Polym Plast Tech Eng* 2007, 46, 305-310.

4.   Morshedian, J.; Hoseinpour, M. P., Polyethylene Cross-linking by Two-step Silane Method: A Review. *Iranian Polymer Journal* 2009, 18, (2), 103-128.

5.   Morshedian, J.; Hoseinpour, P. M., Polyethylene Crosslinking by Two step silane Method: A Review. *Iranian Polymer Journal* 2009, 18, 103-128.

6.   Barzin, J.; Aziz, H.; Morshedian, J., Preparation of Silane-Grafted and Moisture Cross-lInked Low Density Polyethylene: Part I: Factors Affecting Performance of Grafting and Cross-Linking. 2006, 45, 979-983

7.   Forsyth, J. C.; Baker, W. E.; Russell, K. E.; Whitney, R. A., Peroxide-Initiated Vinylsilane Grafting: Structural Studies on a Hydrocarbon Substrate. *Journal of Polymer science: Part A: polymer chemistry* 1997, 35, 3517-3525.

8.   Spencer, M.; Parent, S.; Whitney, R., Composition distribution in poly(ethylene-graft-vinyltrimethoxysilane). *Polymer* 2003, 44, 2012-2023.

9.   Weaver, J. D.; Chowdhury, A. K.; Mowery, D. M.; Esseghir, M.; Cogen, J. M.; Chaudhary, B. I., Grafting of silane-functionalized nitroxyl to polyethylene. *Journal of polymer science: Part A: Polymer chemistry* 2008, 4542-4555.

10.   Willker, W.; Leibfritz, D.; Kerssebaum, R.; Bermel, W., GRADIENT SELECTION IN INVERSE HETERONUCLEAR CORRELATION SPECTROSCOPY. *Magnetic Resonance in Chemistry* 1993, 31, (3), 287-292.

11.   Williamson, R. T.; Marquez, B. L.; Gerwick, W. H., Use of H-1-N-15 PEP-HSQC-TOCSY at natural abundance to facilitate the structure elucidation of naturally occurring peptides. *Tetrahedron* 1999, 55, (10), 2881-2888.

12.   Wang, Y.; Yang, C.; Tomasko, D., Confocal microscopy analysis of supercritical fluid impregnation of polypropylene. *Ind. Eng. Chem. Res.* 2002, 2002, (41), 1780-1786.

13.   Liu, T.; Hu, G.-H.; Tong, G.-s.; Zhao, L.; Cao, G.-p.; Yuan, W.-k., Supercritical carbon dioxide assisted solid-state grafting process of Maleic anhydride onto Polypropylene. *Ind. Eng. Chem. Res.* 2005, 44, 4292-4299.

14.   Li, D.; Han, B.; Liu, Z., Grafting of 2-Hydroxyethyl methacrylate onto Isotactic poly(propylene) using supercritical CO2 as a solvent and swelling agent. *Macromo. Chem. Physic.* 2001, 202, 2187-2194.

CHAPTER 2

STUDY OF SILYLAMINES USING STRUCTURE/PROPERTY

RELATIONSHIPS FOR CO_2 CAPTURE

Background

The transfer of new carbon capture technologies from academia to industry will be cost driven. It is imperative to develop carbon dioxide capture strategies that are efficient from relatively small to large scale. Ultimately, we seek technologies that provide the maximum capture capacity and can be fitted to existing coal-fired power plants with the minimum capital cost and energy requirement. There have been many approaches to address this issue – physical and chemical absorption using solvents, swing adsorption with MOF's, zeolites, membrane technology and chemical looping to name a few. An extensive review of the various methods available for CO_2 capture is given by Olajire et al[13] and brief summary can be found in Table . Pre-combustion capture was given an initial thrust by the government funding, and has led to the realization that post-combustion may be more effective for the immediate future[14].

Flue gas capture from coal-fired plants has traditionally been scrubbed of CO_2 using amine mixtures such as monoethanolamine (MEA). Although this process is popular commercially, it is disadvantageous because an additional solvent (up to 70%), usually water, is required for processing. This results in high operating costs arising mostly from the heating of the solvent rather than the regeneration of the amine. House et al[15] define energy penalty as the fraction of fuel input that must be dedicated to perform each of the CCS steps for a fixed quantity of work output. The most likely efficiency scenario indicates that offsetting the energy penalty incurred from capturing and storing 80% of U.S. coal fleet CO_2 emissions will require an additional 15-20% reduction in overall electricity usage.

Table : Post-combustion capture technologies

CO$_2$ Capture Technology	Pros	Cons
Amine scrubbing	• Mature Technology • High CO$_2$ purity	• Energy penalty • Corrosion
Physical absorption	• Low utility consumption	• Hydrocarbons are co-absorbed
Membrane Technology	• Low regeneration energy • Modular design	• Fouling • Technology in nascent stage
Chemical Looping	• Small energy penalty	• No large scale demonstration

Reversible ionic liquids were designed to minimize, if not eliminate, the need for a co-solvent while maximizing CO$_2$ capture by combining chemical and physisorption mechanism. Reversible solvents can change properties upon application of an external stimulus (Figure). We have developed novel silyl-amine molecules for CO$_2$ capture at the Eckert-Liotta group at Georgia Tech. These novel solvents are neutral molecules (will be referred to as molecular liquids) that react with CO$_2$ to form an ionic liquid, which can further absorb additional CO$_2$ by a physisorption mechanism. As conventional ionic liquids, formed reversible ionic liquids, are capable of physisorbing more CO$_2$ thus increasing the overall capacity of these systems. It is important to note that clean CO$_2$ is obtained upon reversal. The property changes associated with

the transition are drastic and can be used to address the limitations of alkanolamines. Apart from CO_2 capture applications, we have demonstrated the potential of these systems for the extraction of hydrocarbons from oil sands[16] and ease of separation for two reactions – Claisen-Schmidt condensation and Heck coupling[17].

Figure : Reaction scheme of reaction of ionic liquids with CO_2

The unique advantage of these systems is that they can be used in a neat form, without a solvent, and thus have a reduced energy penalty that is required to heat up the ethanol-water mixtures. The presence of silicon lowers the viscosity of these room temperature ionic liquids – silicon has lower electronegativity than carbon and Si—C bond length are substantially longer than the analogous C-C single bonds[18]. Subsequently, modest elevations in temperature reverse the reaction and, in principle, yield pure CO_2 for sequestration (Figure).
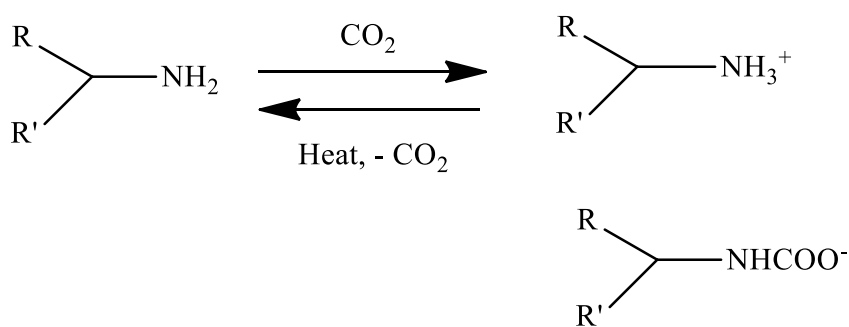
Figure : Equilibrium reaction of silylamines with CO_2

Figure below describes the iterative procedure that is followed to design new molecules for CO_2 capture. We have investigated a series of structure/property relationships by changing

49

the 'R' groups and the length of the alkyl chain attached to the amine. The molecular liquids were synthesized in our labs, and more details are provided in the next section. Efficient scale-up for pilot plant simulations are given due consideration at various steps of synthesis. A variety of analytical techniques - Gravimetry, DSC, TGA, FTIR, Viscometry, and Refractive Index - were used to obtain important process parameters. These properties were used to formulate structure/property relationships which are used to further design new molecules for CO_2 capture.
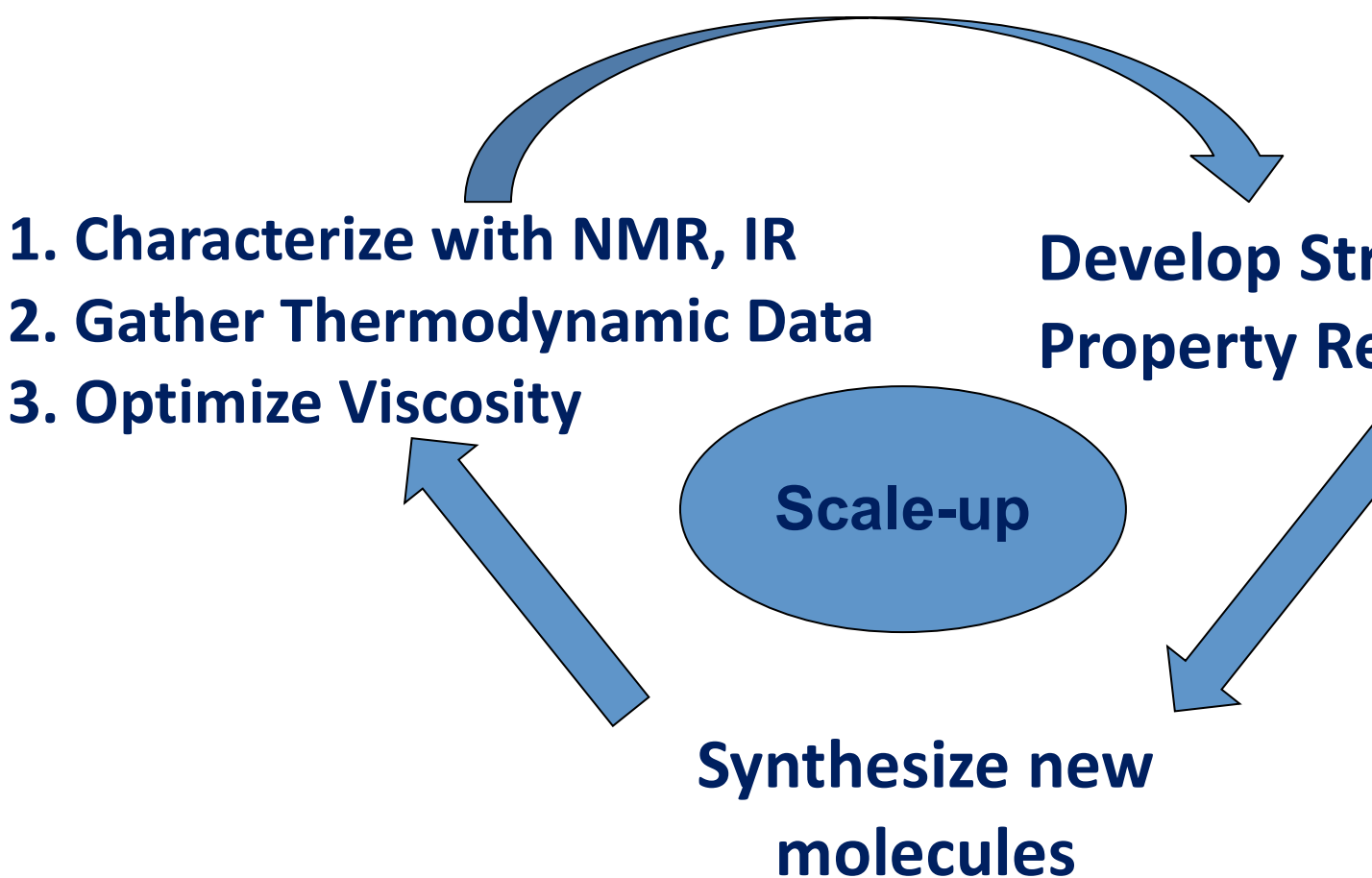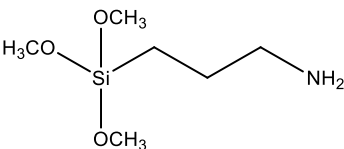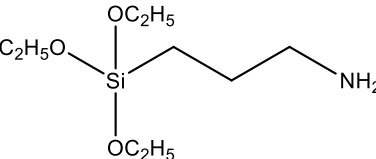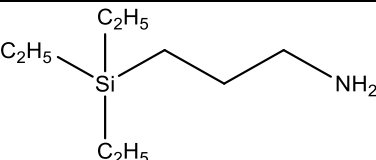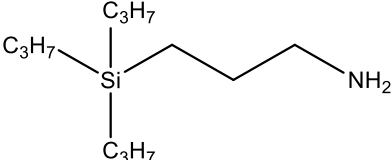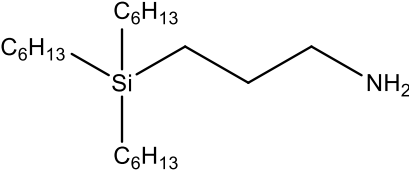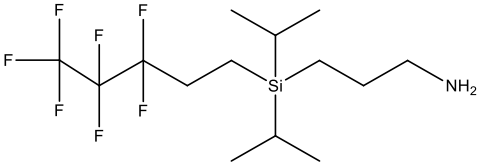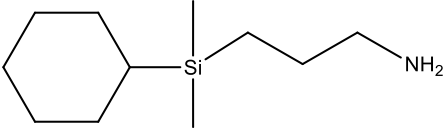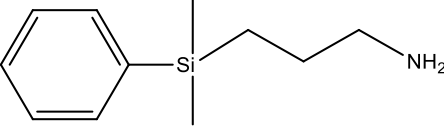
Figure : Iterative procedure for the design of novel solvents

The library of amines synthesized and used for CO_2 capture is given in
.

Table : List of silylamines investigated

Compound	Molecular liquid	Structure	Acronym
1	(3-aminopropyl) trimethoxysilane		TMSA
2	(3-aminopropyl) triethoxysilane		TESA
3	(3-aminopropyl) triethylsilane		TEtSA
4	(3-aminopropyl) tripropylsilane		TPSA
5	(3-aminopropyl) trihexylsilane		THSA

6	(3-aminopropyl) diisopropyl(1H,1H,2H,2H-perfluoropentyl)silane		FSA
7	(3-aminopropyl) cyclohexyldimethylsilane		CHDMSA
8	(3-aminopropyl) phenyldimethylsilane		PDMSA

Experimental

Materials and methods

Triethylsilane (99%), tripropylsilane (99%), trihexylsilane(98%), allylamine(98%), platinum-divinyltetramethylsiloxane (2% in xylenes), Cyclohexyldimethylsilane (98%), Dimethylphenylsilane (98%) and toluene (anhydrous, 99.8%) were purchased from Sigma Aldrich and used without further purification. (3-aminopropyl) trimethoxysilane (97%, TMSA) and (3-aminopropyl) triethoxysilane (98%, TESA) were also sourced from Sigma Aldrich and used from the bottle in the reaction with CO_2. All amines and starting materials for the syntheses were stored in the controlled N_2 atmosphere. N_2 and CO_2 cylinders were obtained from Airgas with purity >99.99%.

Gravimetry and Preparation of the Ionic Liquid:

The weight gain of the molecular liquids after reaction with CO_2 was performed in a sealed vial. A dram vial was sealed with a septum and tape and weighed after purging with nitrogen or argon. A known amount of molecular liquid was injected into the vial and initial weight was recorded. A SS needle connected to a CO_2 cylinder via a flowmeter. The use of flowmeter enabled the introduction of CO_2 gas (at 1 bar) at a constant flow rate for every experiment. The net weight gain of the molecular liquid represents the conversion of the silylamine to ionic liquid and physisorption.

Attenuated Total Reflectance Fourier Transform Infra Red Spectroscopy (ATR-FTIR):

Equilibrium measurements were performed with pre-formed ionic liquid by using a custom-designed and built ATR FT-IR high pressure reactor. A Specac, Ltd. heated Golden Gate attenuated total reflectance (ATR) accessory with diamond crystal and zinc selenide (ZnSe)

focusing lenses was used for the room temperature collection of the molecular and ionic liquid spectra.

Refractive Index (RI):

The refractive indices of both the molecular and the ionic liquid forms were measured using a Reichert Arias 500 Abbe-style refractometer, connected to a circulated cooling bath with glycol as the heat transfer fluid, enabling measurements from 0°C to 75°C. Refractive index measurements are reliable to ±0.0002 at a given temperature, require <0.1 mL of the sample and about five minutes from application time to cleanup and are a convenient analytical tool to quantify conversion of ionic liquid.

Viscometry:

Viscosities were measured using a Rheosys Merlin II cone and plate viscometer. Shear rates were adjusted using trial and error between 10 s^{-1} and 2000 s^{-1} and the final viscosities reported were the average of five values.

Differential Scanning Calorimetry (DSC):

DSC measurements were performed in triplicate with a Q20 TA DSC Instrument. Temperature was ramped from -40°C to 400°C at a ramp rate of 5°C/min. The liquid was sealed in pans using standard crimping procedures and were used for the measurements. The purge gas used was nitrogen.

Results and Discussion:

gives the list of ionic liquids that were designed during the course of the project. Compounds 1 & 2 have moisture-sensitive methoxy and ethoxy groups which made handling under normal working conditions difficult. Compounds 3, 4 & 5 were designed to make more

robust analogues of 1 & 2. This was done by replacing the groups on the silicon with stable alkyl groups. Compound 6 was prepared to study the effect of CO_2-philic fluorine groups on CO_2 capture. All compounds 1-6 yield a liquid/gel at room temperature on reaction with CO_2 which is very important from point of view of replacing MEA solutions in existing power plants. To investigate the effect of asymmetry on the silicon and attaching bulky side groups, compounds 7 & 8 were prepared. However, they turned into a solid on reaction with CO_2 and thus, further research on them was discontinued. For purpose of this chapter, we will concentrate on data from 3, 4 & 5 mostly and 6 whenever data are available.

Synthesis of molecular liquids:

Compounds 1 & 2 are commercially available and were used as purchased. Compounds 3, 4, 5 & 6 were prepared via the efficient, one step hydrosilylation reaction of allylamine with tri-alkylsilane using Pt-DVDS as the catalyst with toluene as the solvent (Figure , Figure). The pure molecular liquids were purified using vacuum distillation and were stored in the glovebox and used as required.
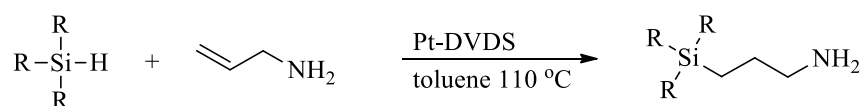
R=ethyl,propyl,hexyl

Figure : One step scalable reaction for synthesis of Compounds 3, 4, 5
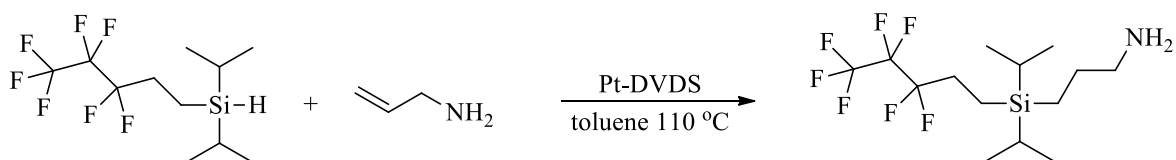
Figure : One-step reaction for the synthesis of Compound 6

Compounds 7, 8 were synthesized from silane starting materials (cyclehexyldimethylsilane and phenyldimethylsilane) as shown in Figure 4 and after preliminary characterization, were not studied further.

Reversibility of the switch

The reversibility of the switch between the neutral and the ionic liquid form was studied using ^{13}C NMR (Figure) by sparging ^{13}C-labeled-CO_2 through the molecular liquid of TPSA. The appearance and disappearance of the carbon of the -NHCOO$^-$ peak at 165 nm is conclusive evidence for the switch. The peaks below 50 nm are the carbons on the alkyl chains on the ionic (IL) and the molecular liquid (ML). The triplet at ~77 nm is the carbon on the deuterated chloroform used as the solvent for NMR.
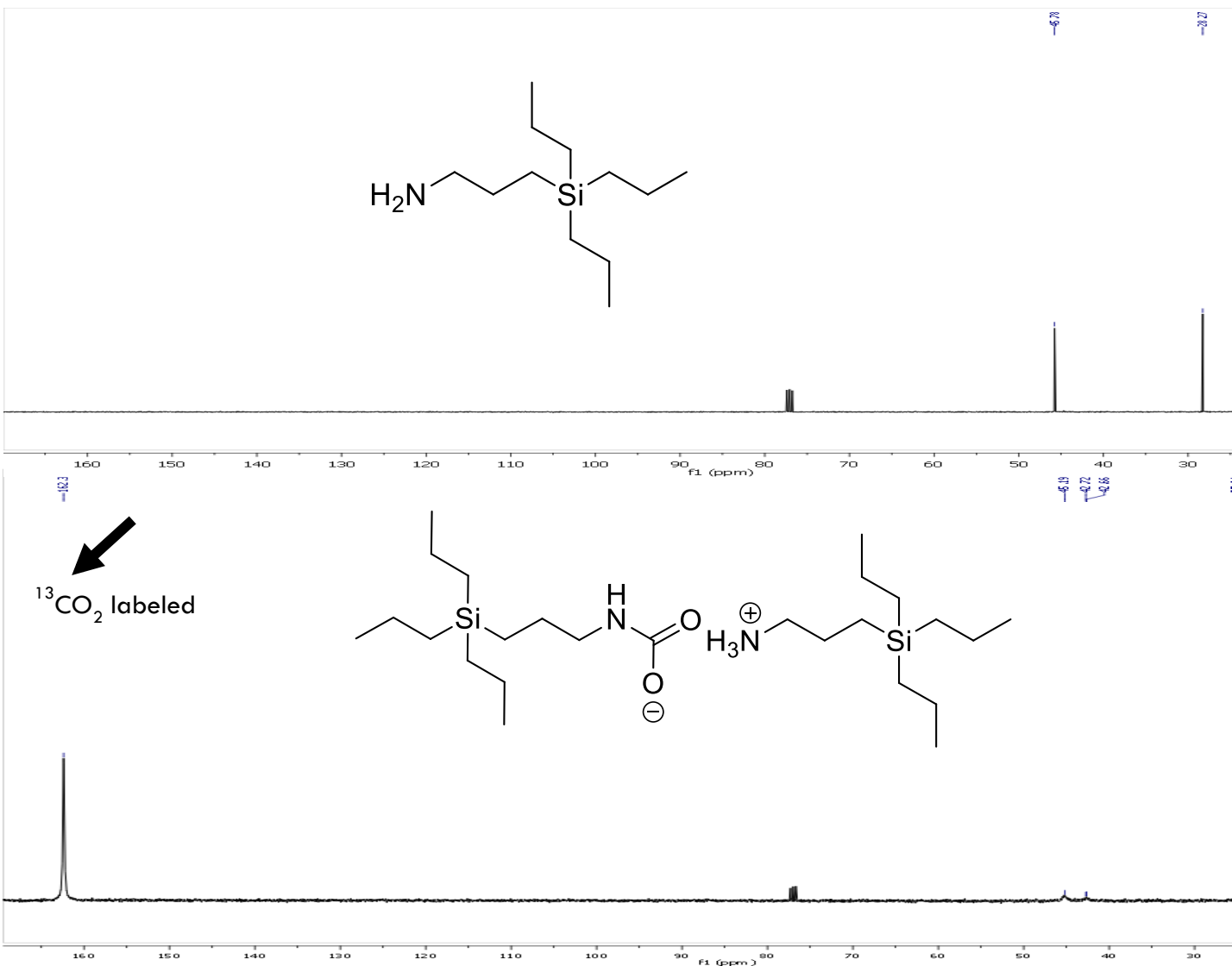
Figure : ^{13}C NMR of the TPSA ML and IL

CO$_2$ Capture Capacity:

The theoretical CO$_2$ capacity, for all amines (1-8) is the same on a mol CO$_2$/mol amine (=0.5) basis because the reaction is the same. Experimentally, the overall capacity was determined using gravimetry and has two components – complete conversion by chemical reaction and physisorption at 1 bar. The excess capacity, after accounting for chemisorption, was taken as the contribution of physisorption. The physisorption component would be highly significant for CO$_2$ capture at higher pressures (of order of 50 bar), and this could make

silylamines attractive for separation of CO_2 from natural gas. More discussion about the physisorbed CO_2 is given in next section.

The molecular weight of the amine increases from TEtSA to TPSA to THSA and the capacity on a mol CO_2/kg amine basis decreases from 2.89 for TEtSA to 1.46 for THSA (Figure). All compounds are similar or better than 70% water - 30% MEA solution with a 2.46 mol CO_2/kg amine as the theoretical capture capacity.
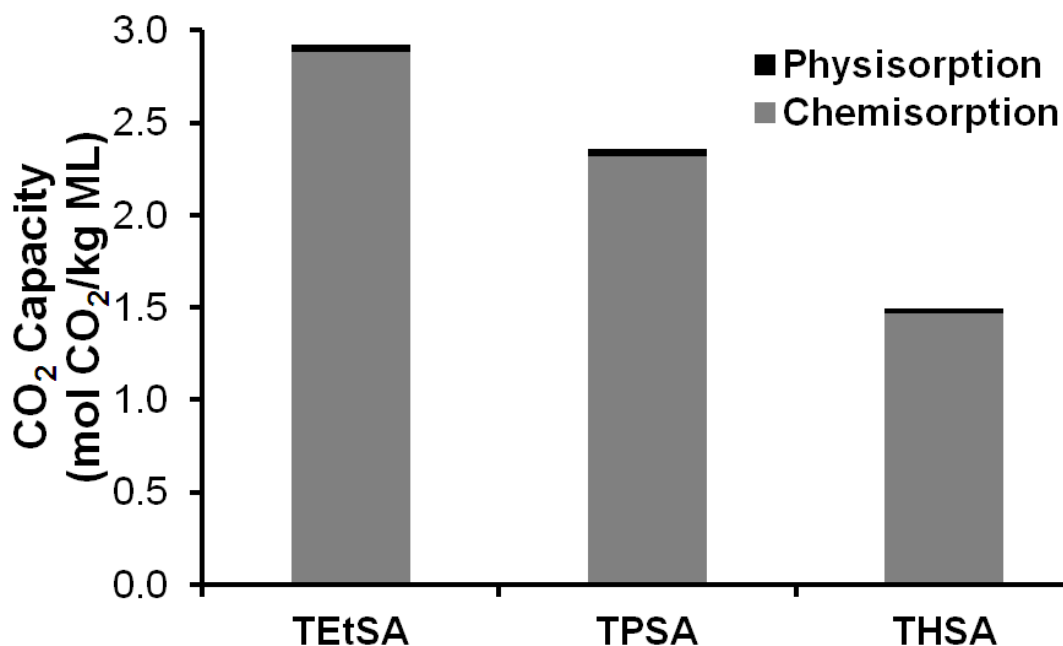
Figure : Capture capacities of silylamines

Evidence for Physisorbed CO_2 using FTIR:

There are two regions in the IR spectrum that were used for determining molecular and ionic liquid mole fractions: the broad ammonium stretch vibration between 3100-2600 cm^{-1} and the C=O stretch from the carbamate between 1740-1520 cm^{-1}. These are represented as Regions I and III in the Figure , respectively. The asymmetric C=O stretch of the CO_2 molecule is seen at 2350 cm^{-1} (in Region II) and helps to identify the presence of physisorbed CO_2 in the sample of preformed ionic liquid.
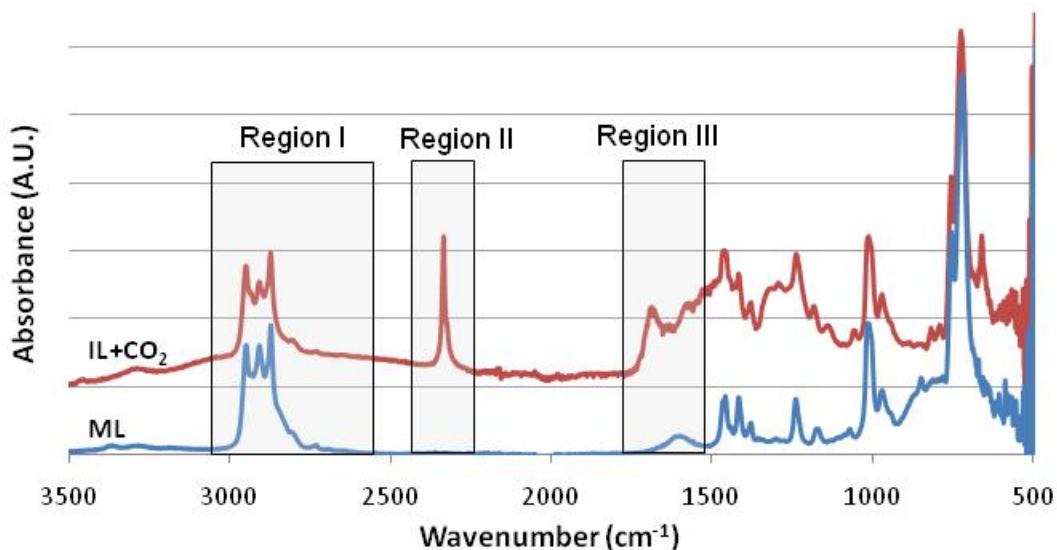
Figure : Infra Red spectra of molecular and ionic liquid of TPSA

Quantitative Relationship between Refractive Index and Conversion:

The refractive index difference between the molecular liquid and the ionic liquid samples is approximately 0.02 for a specific structure at a fixed temperature. Literature favorably propounds the use of a mixing rule such as Lorentz Lorentz for correlating Refractive Index for binary mixtures consisting of ionic liquid and an organic solvent[19]. Lorentz Lorentz (LL) mixing rule applied to a binary solution is as follows:

$$\frac{n_{12}^2 - 1}{n_{12}^2 + 2} = \phi_1 \frac{n_1^2 - 1}{n_1^2 + 2} + \phi_2 \frac{n_2^2 - 1}{n_2^2 + 2} \qquad ()$$

Where n_{12} is the refractive index of the mixture, n_i is the refractive index of the pure species, and Φi corresponds to the volume fraction of that species,

$$\phi_1 = \frac{x_1 v_1}{\sum_i x_i v_i} \qquad ()$$

where x is the mole fraction and v is the molar volume of component i.

The mixing rules when applied to our system yielded the following graph (Figure) which was initially used predicting conversion. From the nature of the graph, it can be easily seen that the relationship is exponential. Simultaneously, experiments were conducted to quantify conversion and establish the relationship in a concrete manner.
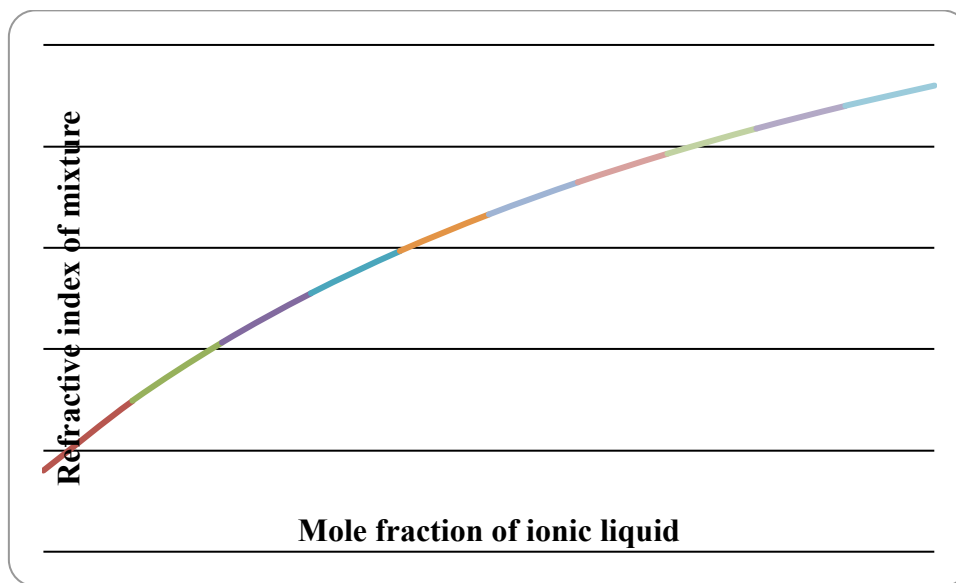
Figure : Predicting conversion from LL rules

Many samples with varying degrees of conversion of molecular liquid were prepared and the RI of the samples was measured immediately. Conversion was calculated using gravimetric technique – By determining the net weight gain of the molecular liquid on reaction with CO_2 as was discussed earlier. Figure shows the refractive index of system TPSA as a function of conversion at 25°C and it is clear that the relationship is closer to being linear than exponential. The refractive index of the pure ML and RevIL for TPSA are 1.4540 and 1.4732 respectively at 25°C. The pure ML TPSA shows a refractive index of 1.4540, which increases linearly up to 1.4732 for the totally converted RevIL. The relationship between RI and conversion is found to be linear from experiments with TPSA and TEtSA and it is anticipated that the trend will hold for other silylamines as well. To conclude this study, the refractive index can be used as a

quantitative measure of conversion from ML to RevIL, enabling us to investigate a wide range of properties as a function of the conversion using RI as the analytical technique.

y = 0.0209x + 1.4203
R² = 0.92027

Refractive Index (y-axis)

Conversion (x-axis)
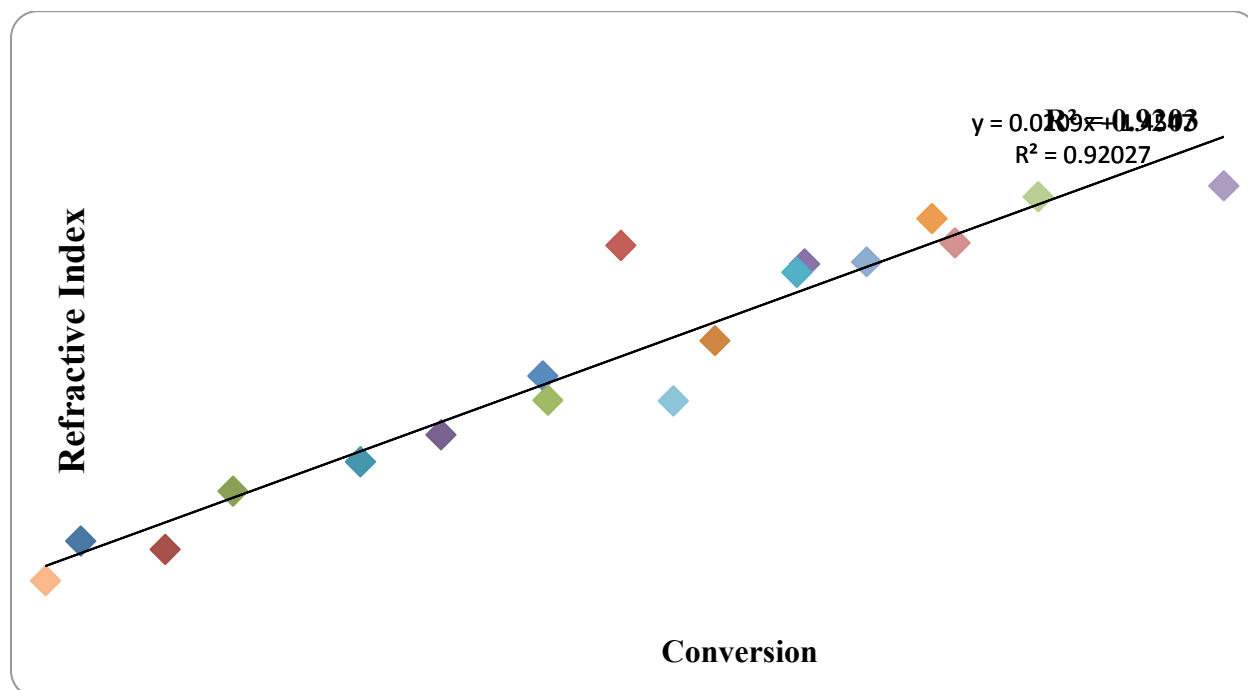
Figure : Refractive index measurements as a function of conversion for TPSA

Recyclability of the switch

It was demonstrated that this reversible reaction can be carried on for multiple cycles, making the amine reusable in the industry for CO_2 capture. The recyclability of the switch was demonstrated using refractive index for five cycles. For TPSA, the molecular liquid was reacted with CO_2 at 1 bar for 75 mins to form the ionic liquid. Once that is done, the ionic liquid was heated at 100°C for 1 hour to obtain the molecular liquid. Refractive index was used to monitor the reaction and reversal continuously and was plotted in the figure below. RI of the molecular liquid of TPSA is 1.454 and that of the ionic liquid is 1.473. The NMR of the molecular liquid was taken after 5 cycles and compared to the ^{1}H NMR of the original molecular liquid. No visible molecular degradation was seen. We expect the silylamines to have continued reactivity for many more cycles than what is demonstrated here.
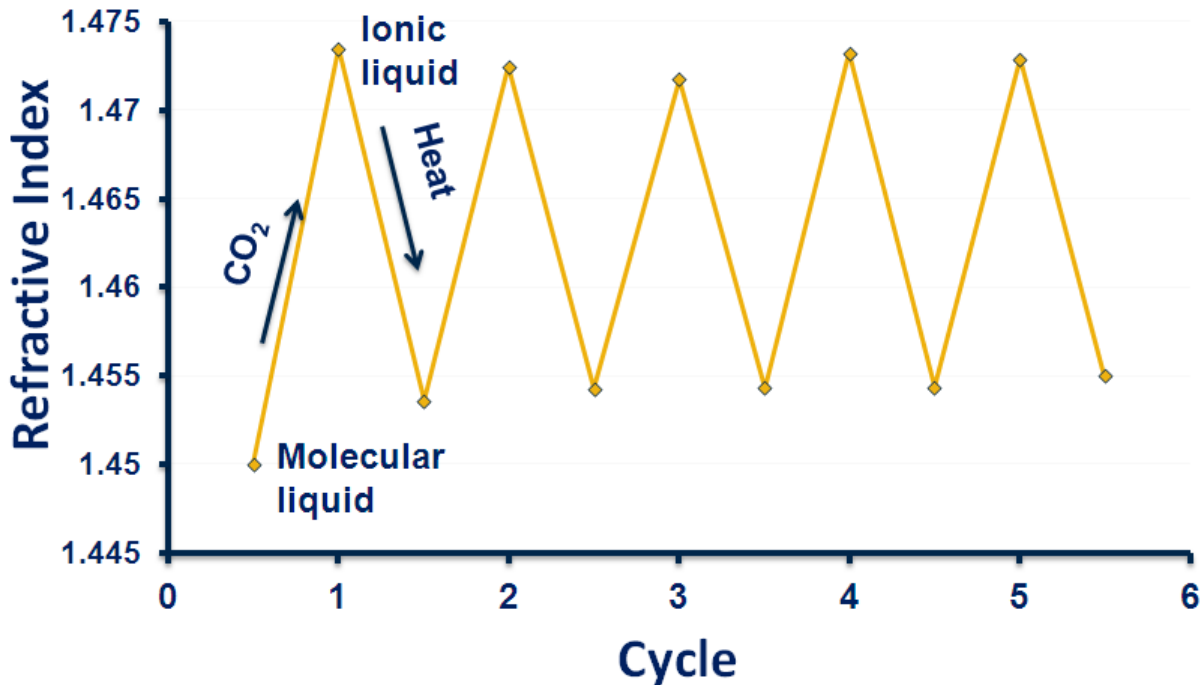
Figure : Recyclability of the switch for five cycles

Viscosity of Ionic Liquids and Methods to Control it:

The most common problem with conventional room temperature ionic liquids is the increase of viscosity on reaction with CO_2. Brennecke and coworkers[20] have used molecular modeling to study the ionic liquids. Atomistic molecular dynamics trace this viscosity increase to the formation of a pervasive network of salt bridges between the positive and negative ions.

The viscosity of the silylamines in their neutral form is less than 50cP. As seen in Table , the TEtSA ionic liquid has a viscosity of 7600 cP at 25°C while it decreases to 1650 cP for THSA. By adding more alkyl chains on the silicon, the viscosity has reduced systematically from TEtSA to TPSA to THSA. This might be because the ions are farther apart from each other in the network formed by the ammonium bicarbonate ions. Viscosity of FSA is much higher; and it was developed to study structure/property relationships only.

Also, the viscosities at 40°C, which are closer to flue gas conditions than 25°C, are much lower. The viscosity of THSA at 40°C is 500 cP. The target viscosity for keeping the processing costs minimum from the industry standpoint is 100 cP.

Table : Viscosities of silylamines

Compound	Viscosity @ 25°C (cP)	Viscosity @ 40°C (cP)
TEtSA	7600	2000
TPSA	4000	1050
THSA	1650	500
FSA	12300	2900

Viscosity was found to be a function of conversion. Two distinct regions were identified (Figure). In region 1 (shown in the inset), the viscosity of the ionic liquids was fairly low and varied slightly with conversion. In region 2, the viscosity increase was highly dependent upon conversion. It has to be noted that measuring viscosity with an instrument of higher accuracy at the lower viscosity region would provide more insight into the behavior in region 1.

The viscosity of the TPSA ML is below 50 cP. The viscosity of the ionic liquids stays fairly low (~300 cP) until the 75% conversion. Further reaction results in a drastic increase of viscosity of 4000 cP, the value for a fully formed IL.
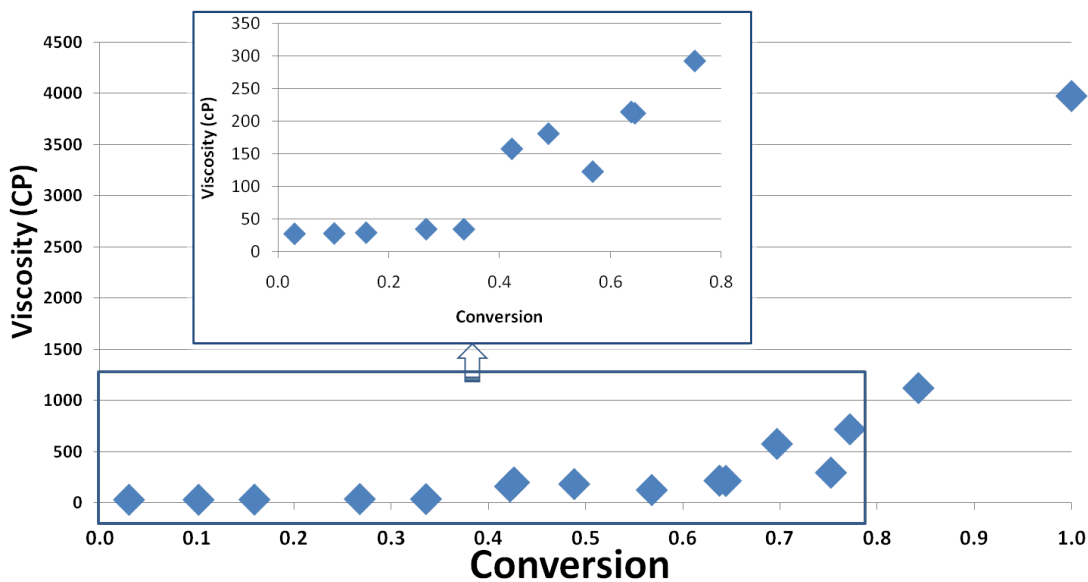
Figure : Viscosity as a function of conversion for TPSA; region 1 shown in the inset

A similar set of experiments was performed on TEtSA. Two regions were again identified. Viscosity was below 300cP up to 70% conversion and it increased to 7000cP for the fully formed ionic liquid (Figure).
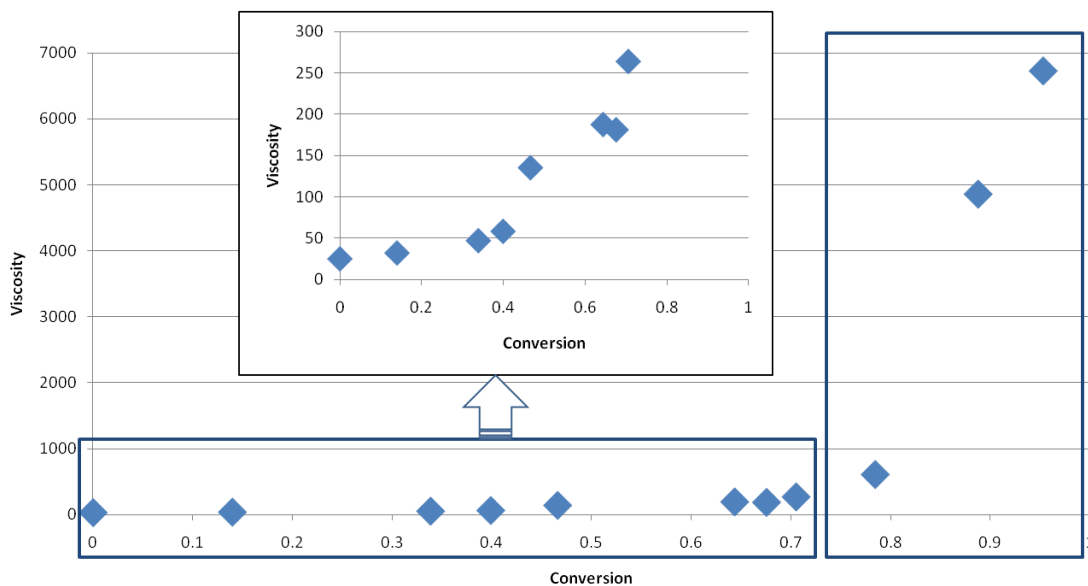
Figure : Viscosity as a function of conversion for TEtSA; region 1 shown in inset

While these viscosity results are not yet less than 100 cP, significant lowering of viscosity of the completely formed ionic liquid has been made. Viscosity can be lowered by 1) Adding 'R' groups on the silicon 2) By increasing the temperature 3) By lowering the conversion and using Region I as the working range. Small amounts of water in the flue gas also help to reduce the viscosity of the system and the interaction of water with the silylamines is currently being studied. Improvements to viscosity are further being made by designing molecules which have steric hindrance around the amine i.e. addition of methyl groups on the carbon adjacent to the NH_2.

Two important properties from DSC - Reversal temperature and Boiling point of silylamines

On the DSC thermogram for an ionic liquid, there are typically two events - reversal of the ionic liquid to give the molecular liquid and evaporation of the molecular liquid - as shown in Figure . The reversal temperatures obtained from DSC's are the onset of the reversal event. The average reversal temperature decreases (Figure) as we increase the size (chain length) of our substituent groups, from 70.6°C for TEtSA to 50.6°C for THSA. The reason for this is the increasing entropic effects due to the increasing size of the substituent groups. FSA also has a low T_{rev} of 53.6°C due to the lengthy fluorinated chain attached to the Si. It has to be noted that this is the temperature at which the reversal begins and the rate of reversal is higher at higher temperatures. Industrially, MEA solutions are heated to 100-120°C to obtain the CO_2 and to recycle them.
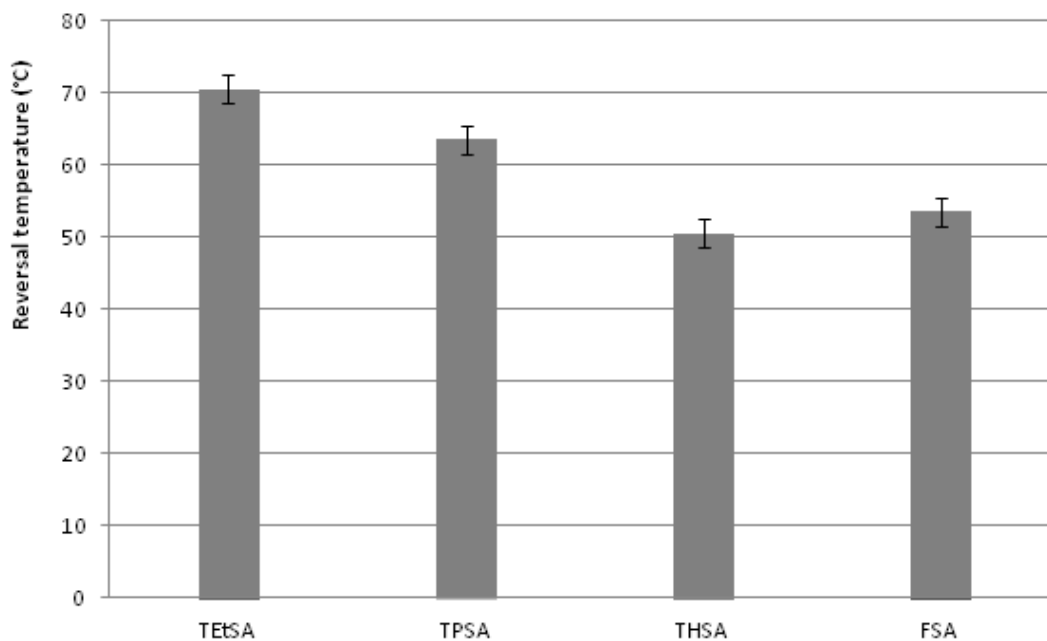
Figure : Reversal temperatures for compounds 3-6
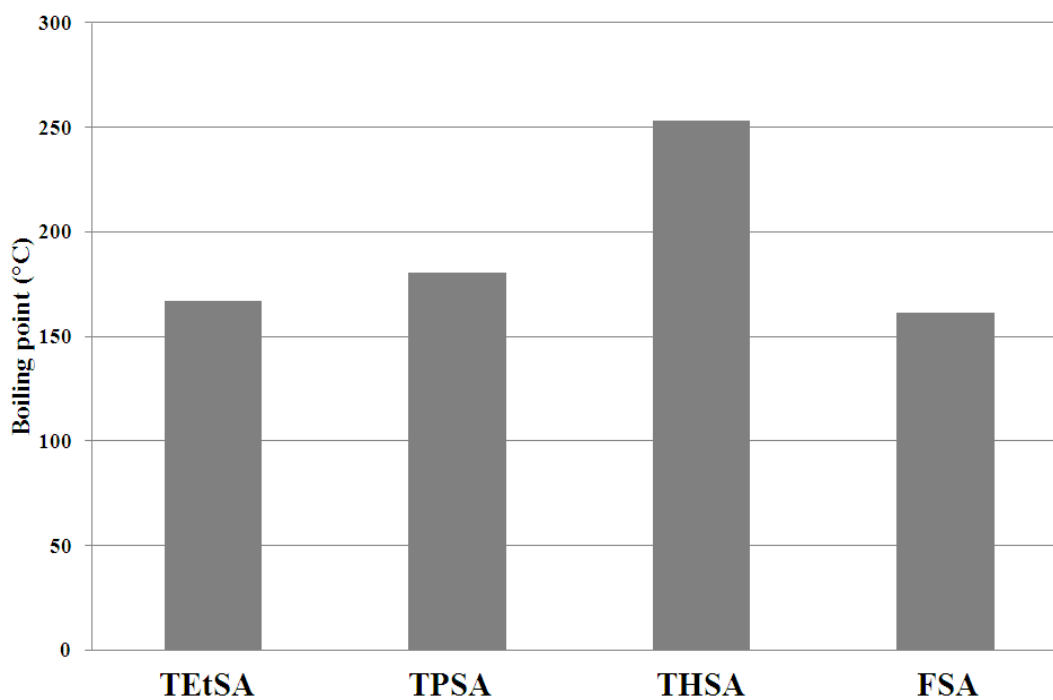
Figure : Boiling points of the silylamines

The heat of reaction was obtained by integrating the area under the first curve and it was

~105KJ/mol (all values within experimental error) for all silylamines discussed in Figure . This

is because the reaction between the amine and the CO_2 is the same in all cases irrespective of the amine. The onset of the evaporation curve on the DSC is noted as the boiling point of the silylamine and it increases from 167°C to 253°C from TEtSA to THSA (Figure). This increase is consistent with the increase of molecular weight of the amine.

As we move from TEtSA to TPSA to THSA, the two events on the DSC move farther apart from each other as depicted in Figure . This is beneficial because the solvent vaporization is minimized during the reversal event and reduces the make-up costs of the amine.
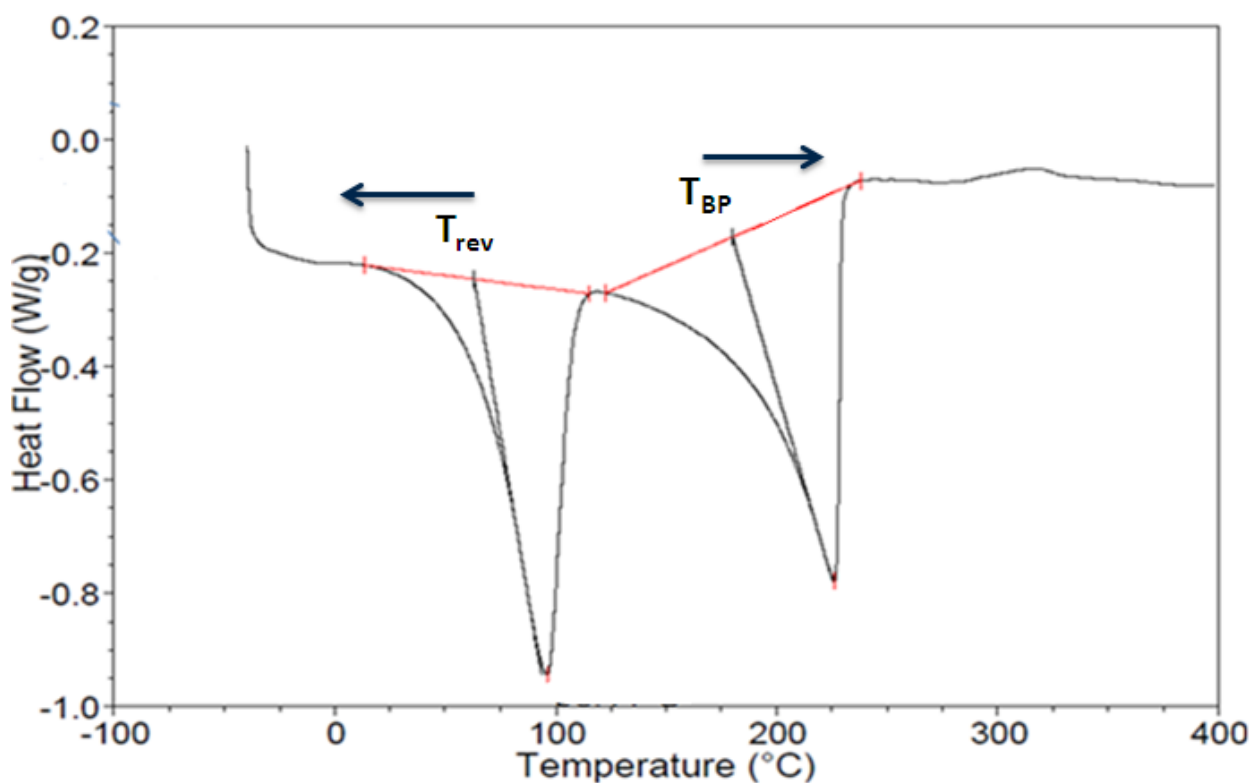
Figure : DSC thermogram of a typical ionic liquid. Figure shows TPSA

Interaction of SO₂ with silylamines:-

Some coals can contain several percent of sulphur and combustion of these coals can result in oxides of sulphur in the flue gas stream. Heldebrandt et al[21] recently reported the formation of SO_2 binding organic liquids which react in a reversible manner similar to silylamines. Silylamines react with SO_2 in the same manner in an analogous manner to CO_2, resulting in the formation of ammonium and sulfamate ions (Figure).
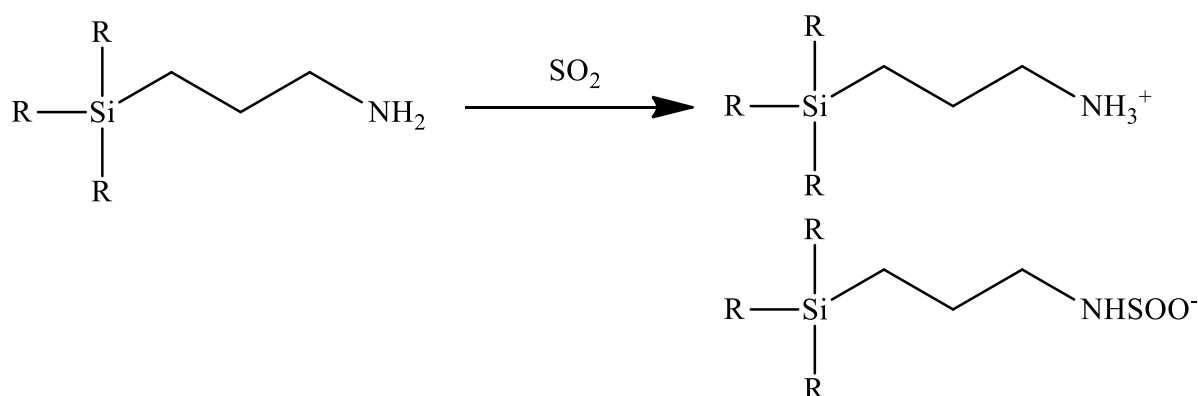
Figure : Reaction of silylamines with SO₂

The SO_2 absorption capacity, similar to CO_2 capacity, was investigated using gravimetric measurements with TPSA. Based on stoichiometry alone, the expected number of moles of SO_2 per mole of TPSA ML is 0.5.
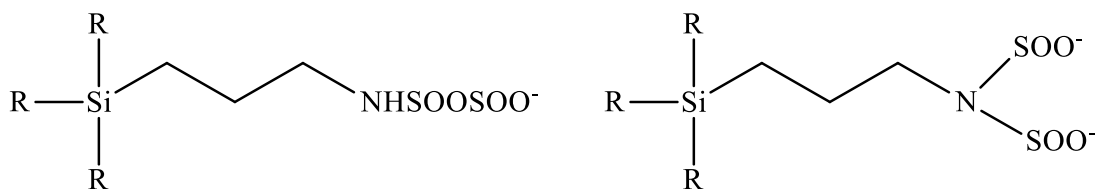
Figure : Additional possible side products on reaction of SO₂ with silylamines

Experimentally, the value was found to be 1.592 and is much more than what was expected. This increased uptake can be attributed to physisorption and/or the formation of additional side products between SO_2 and TPSA as shown in Figure . Additional research is

ongoing with simulated flue gas streams containing both SO_2 and CO_2 and more details can be obtained from the thesis of a former group member[22].

Summary:

An overview of the key properties of the silylamines that we have investigated so far is given in

.

Table : Summary of key properties

Compound	Mol. Wt	Theoretical Capacity (mol CO_2 /kg amine)	IL viscosity (cP) at 25 ^{o}C	Reversal Temp. (^{o}C)	Heat of Reaction (kJ/mol)	ML Boiling Point (^{o}C)
3 (TEtSA)	173	2.89	7600	71	104	167
4 (TPSA)	215	2.32	4000	64	114	180
5 (THSA)	342	1.46	1650	51	108	253
6 (FSA)	369	1.35	20,000	53.6	109	161

Conclusions:

Coal-fired utility boilers generate nearly 50% of the electricity in the United States. Therefore, for the foreseeable future, coal will continue to be the most important source of energy while we develop alternatives like nuclear and hydrothermal to take on the load. Greenhouse emissions are an accompanied disadvantage and carbon capture and sequestration is becoming more of a necessity now. MEA is the most commonly chosen solvent so far, and is the benchmark for research and development efforts for solvents for post-combustion CO_2 capture.

We have developed silylamines for CCS through an iterative procedure using studying structure/property relationships systematically. As we go from TEtSA to TPSA to THSA, the viscosity of the ionic liquid decreases to our advantage. Viscosity of the ionic liquid can be kept at the minimum by: 1) Using a lower conversion as the working range 2) By operating at temperatures higher than room temperature as is likely to be the case in the industry during CO_2 capture from flue gas 3) By continuing to design new molecules using the structure/property relationships that we have developed. We already have been successful at the third option by introducing steric hindrance close to the amine and investigations are being completed.

The reversal temperature decreases and boiling point increases which dictates the amount of solvent vaporization that will occur during reversal; THSA has the least overlap between the two events. The molecular weight of the silylamine also increases, leading to the unfavorable decrease in capture capacity. FSA was investigated to understand structure-property relationships only. We find that TPSA has the optimal properties, between TEtSA and THSA, and could be the best silylamine amongst the library of amines (
) studied for cost-effective and energy efficient CO_2 capture from the flue gas of coal-fired power plants.

Path Forward:

Because of the high potential for physisorption of CO_2 in the completely formed ionic liquid, another application that these silylamines could be developed for is the separation of CO_2 from high-pressure natural gas deposits. This could be one of directions of research with support from our industrial partner.

We are in the continual process of updating the library of silylamines. Design, synthesis and characterization of amines with alkyl groups on the propyl chain between the silicon and the amine are underway. These amines are expected to have lower viscosity than the ones discussed in this chapter.

Also, flue gas has components other than CO_2, like H_2O and SO_2 and the interactions of silylamines with these gases have not been completely understood. For example, preliminary studies indicate that water is soluble in small quantities (up to 17 wt % depending on the amine) in the molecular liquid and forms a single-phase with the amine. The presence of water can reduce the viscosity of the solvents as well. Silylamines have a higher affinity for SO_2 than CO_2 and it would be interesting to investigate the reversibility of the reaction in Figure .

References:

1.   (a) Hjertberg, T.; Palmlof, M.; BA, S., Chemical reactions in cross-linking of copolymers of ethylene and vinyltrimethoxysilane. *Journal of applied polymer science* **1991,** *42*, 1185-1192; (b) Pollet, P.; Liotta, C.; Charles\, E.; Verma, M.; Nixon, E.; Sivaswamy, S.; Jha, R.; Momin, F.; Gelbaum, L.; Chaudhary, B. I.; Cogen, J. M., Radical mediated graft modification of polyolefin models with vinyltrimoethoxysilane: A fundamental study. *Industrial and Engineering Chemistry Research* **2011,** (50), 12246-12253.

2.   Barzin, J.; Azizi, H.; Morshedian, J., Preparation of Silane-Grafted and Moisture Crosslinked Low Density Polyethylene. Part II: Electrical, Thermal and Mechanical Properties. *Polym Plast Tech Eng* **2007,** *46*, 305-310.

3.   Morshedian, J.; Hoseinpour, M. P., Polyethylene Cross-linking by Two-step Silane Method: A Review. *Iranian Polymer Journal* **2009,** *18* (2), 103-128.

4.   Morshedian, J.; Hoseinpour, P. M., Polyethylene Crosslinking by Two step silane Method: A Review. *Iranian Polymer Journal* **2009,** *18*, 103-128.

5.   Barzin, J.; Aziz, H.; Morshedian, J., Preparation of Silane-Grafted and Moisture Cross-lInked Low Density Polyethylene: Part I: Factors Affecting Performance of Grafting and Cross-Linking. **2006,** *45*, 979-983

6.   Forsyth, J. C.; Baker, W. E.; Russell, K. E.; Whitney, R. A., Peroxide-Initiated Vinylsilane Grafting: Structural Studies on a Hydrocarbon Substrate. *Journal of Polymer science: Part A: polymer chemistry* **1997,** *35*, 3517-3525.

7.   Spencer, M.; Parent, S.; Whitney, R., Composition distribution in poly(ethylene-graft-vinyltrimethoxysilane). *Polymer* **2003,** *44*, 2012-2023.

8.   Weaver, J. D.; Chowdhury, A. K.; Mowery, D. M.; Esseghir, M.; Cogen, J. M.; Chaudhary, B. I., Grafting of silane-functionalized nitroxyl to polyethylene. *Journal of polymer science: Part A: Polymer chemistry* **2008**, 4542-4555.

9.   Willker, W.; Leibfritz, D.; Kerssebaum, R.; Bermel, W., GRADIENT SELECTION IN INVERSE HETERONUCLEAR CORRELATION SPECTROSCOPY. *Magnetic Resonance in Chemistry* **1993,** *31* (3), 287-292.

10.   Williamson, R. T.; Marquez, B. L.; Gerwick, W. H., Use of H-1-N-15 PEP-HSQC-TOCSY at natural abundance to facilitate the structure elucidation of naturally occurring peptides. *Tetrahedron* **1999,** *55* (10), 2881-2888.

11.   Antosik, M.; Sandler, S. I., Vapor-liquid equilibria of hydrocarbons and tert-amyl methyl ether. *Journal of chemical and engineering data* **1994,** *39*, 584-587.

12.   (a) Wang, Y.; Yang, C.; Tomasko, D., Confocal microscopy analysis of supercritical fluid impregnation of polypropylene. *Ind. Eng. Chem. Res.* **2002,** *2002* (41), 1780-1786; (b) Liu, T.; Hu, G.-H.; Tong, G.-s.; Zhao, L.; Cao, G.-p.; Yuan, W.-k., Supercritical carbon dioxide assisted solid-state grafting process of Maleic anhydride onto Polypropylene. *Ind. Eng. Chem. Res.* **2005,** *44*, 4292-4299; (c) Li, D.; Han, B.; Liu, Z., Grafting of 2-Hydroxyethyl methacrylate onto Isotactic poly(propylene) using supercritical CO2 as a solvent and swelling agent. *Macromo. Chem. Physic.* **2001,** *202*, 2187-2194.

13.   Olajire, A., CO2 capture and separation technologies for end-of-pipe applications - A review. *Energy* **2010,** *35*, 2610-2628.

14.   Rameshni, M., Carbon Capture Overview. **2010**.

15.   House, K. Z.; Harvey, C.; Aziz, M.; Schrag, D., The energy penalty of post-combustion CO_2 capture & storage and its implications for retrofitting the U.S installed base. *Energy & Environmental Science* **2009,** *2*, 193-205.

16.   Blasucci, V.; Hart, R.; Mestre, V. L.; Hahne, D. J.; Burlager, M.; Huttenhower, H.; Thio, B. J. R.; Pollet, P.; Liotta, C.; Eckert, C., Single component, reversible ionic liquids for energy applications. *Fuel* **2010,** *89*, 1315-1319.

17.   Hart, R.; Pollet, P.; Hahne, D. J.; John, E.; Mestre, V. L.; Blasucci, V.; Huttenhower, H.; Leitner, W.; Eckert, C.; Liotta, C., Benign coupling of reactions and separations with reversible ionic liquids. *Tetrahedron* **2010,** *66*, 1082-1090.

18.   Shirota, H.; Castner, E., Why are the viscosities lower for ionic liquids with -$CH2Si(CH3)3$ vs -$CH2C(CH3)3$ substitutions on the imidazolium cations. *Journal of Physical Chemistry* **2005,** *109*, 21576-21585.

19.   Iglesias-Otero, M. A.; Troncoso, J.; Carballo, E.; Romanı, L., Density and refractive index in mixtures of ionic liquids and organic solvents: Correlations and predictions. *J. Chem. Thermodynamics* **2008,** *40*, 949-956.

20.   E, G. K.; Maginn, E. J., Amine-functionalised task-specific ionic liquids: A mechanistic explanation for the dramatic increase in viscoisty upon complexation with CO_2 from molecular simulation. *Journal of american chemical society* **2008,** *130*, 14690-14704.

21.   Heldebrandt, D. J.; Koech, P. K.; Yonker, C. R., A reversible zwitterionic SO2-binding organic liquid. *Energy and environmental science* **2010,** *3*, 111-113.

22.   Momim, F., Reaction of SO2 with RevIL's for CO2 capture. **2011**.

23.   Ahmad, Z., *Principles of Corrosion Engineering and Corrosion Control*. 2006.

24.	Kladkaew, N.; Idem, R.; Tontiwachwuthikul, P.; Saiwan, C., Corrosion behavior of carbon steel in the Monoethanolamine - H2O - CO2 - O2 - SO2 system: Products, Reaction pathways and Kinetics. *Industrial & Engineering Chemistry Research* **2009,** *48*, 10169-10179.

25.	Barham, H.-A.; Si Ali, B.; Yusoff, R.; Kheirodin Aroua, M., Corrosion of Carbon steel in aqueous carbonated solution of MEA/[bmim] [DCA]. *International Journal of Electrochemical Science* **2011,** *6*, 181-198.

26.	Guo, X.; Y, T., The effect of corrosion product layers on the anodic and cathodic reactions of carbon steel in CO2 saturated MDEA solutions at 100C. *Corrosion Science* **1999,** *41*, 1391-1402.

27.	Veawab, A.; Aroonwilas, A., Identification of oxidising agents in aqueous amine - CO2 systems using a mechanistic corrosion model. *Corrosion Science* **2002,** *44*, 967-987.

28.	(a) Veawab, A.; Tontiwachwuthikul, P.; Bhole, S., Studies of Corrosion and Corrosion control in a CO2-AMP environment. *Industrial & Engineering Chemistry Research* **1997,** *36*, 264-269; (b) Veawab, A.; Tontiwachwuthikul, P.; Chakma, A., Influence of process parameters on corrosion behavior in a sterically hindered amine-CO2 system. *Industrial & Engineering Chemistry Research* **1999,** *38*, 310-315; (c) Veawab, A.; Tontiwachwuthikul, P.; Chakma, A., Corrosion behavior of carbon steel in the CO2 absorption process using aqueous amine solutions. *Industrial & Engineering Chemistry Research* **1999,** *38*, 3917-3924.

29.	Lang, F.; Mason, J. F., Corrosion in amine gas treating solutions. *Corrosion Science* **1958**, 105-108.

30.	Eustaquio-Rincon, R.; Rebolledo-Libreros, M. E.; Trejo, A.; Molnar, R., Corrosion in Aqueous solution of two alkanolamines with CO2 and H2S: N-Methyldiethanolamine + Diethanolamine at 393 K. *Industrial & Engineering Chemistry Research* **2008,** *47*, 4726-4735.

31.   Veawab, A.; Tontiwachwuthikul, P.; Chakma, A., Corrosion behavior in sterically-hindered amine for CO2 separation. *Greenhouse Gas Control Technologies* **1999**, 77-81.

32.   Deyab, M. A., Effect of cationic surfactant and inorganic anions on the electrochemical behavior of carbon steel in formation water. *Corrosion Science* **2007,** *49*, 2315-2328.

33.   Osman, M. M., Hexadecyl trimethyl ammonium bromide as an effective inhibitor for the corrosion of steel in sulphuric acid solution. *Anti-Corrosion methods and materials* **1998,** *45* (3), 176-180.

34.   Driver, R.; J, M. R., Inhibition by n-alkylquaternary ammonium compounds. *British Corrosion Journal* **1980,** *15* (3), 128-131.

35.   Elachouri, M.; Hajji, M. S.; Kertit, S.; Essassi, E. M.; Salem, M.; Coudert, R., Some surfactants in the series of 2-(alkyldimethylammonio) alkanol bromides as inhibitors of the corrosion of iron in acid chloride solution. *Corrosion Science* **1995,** *37* (3), 381-389.

36.   Likhonova, N.; Dominguez-Aguilar, M.; Olivares-Xometl, O.; Nava-Entzana, N.; Arce, E.; Dorantes, H., The effect of ionic liquids with imidazolium and pyridinium cations on the corrosion inhibition of mild steel in acidic environment. *Corrosion Science* **2010,** *52*, 2088-2097.

37.   Eckert, C. A.; Wong, K. F., Vapor-Liquid equilibria of 1,3-butadiene systems. *Journal of chemical and engineering data* **1969,** *14* (4), 432-436.

APPENDIX I

CORROSION BEHAVIOUR OF TRIPROPYLSILYLAMINE (TPSA) FOR CO_2 SEPARATION FROM FLUE GAS
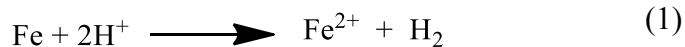
Introduction

Extensive study by the National Association of Corrosion Engineers in 1998 was done to calculate the costs of corrosion in the United States. Results of the study show that the costs of corrosion add up to a staggering $276 billion US dollars. These are the direct costs incurred by owners and operators of structures, manufacturers of products, and suppliers of services. And does not include costs like lost productivity, taxes, overhead etc. The U.S. economy was further divided into various sectors and costs were analyzed per sector. For petroleum refining alone, the costs were $3.7 billion. This included the nation's 163 refineries supplied more than 18 million barrels per day of refined petroleum products in 1996. Maintenance expenses make up $1.8 billion of this total, vessel expenses are $1.4 billion, and fouling costs are approximately $0.5 billion annually. This reflects the significant impact of the corrosion problems in plant operations.[23]

All amine treating plants have experiences of corrosion. Corrosion occurs in many different forms – like general, pitting, stress corrosion cracking. The plant areas most susceptible to corrosion are areas where the acid gas loading and temperatures are high. It is an operating problem because it results in unplanned downtime, production losses and reduced equipment life. In addition to that, corrosion has an adverse impact on the safety of the plant personnel. Often raised is the incident caused due to severe corrosion in the refinery at the Romeoville, IL owned by union oil company resulting in disastrous explosion and fire. An amine absorber pressure vessel ruptured in 1984 and released large quantities of flammable gases and vapors resulting in
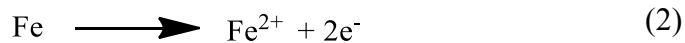
the death of 17 people and damages more than $100 million. Even though no other incident has been reported ever since, this is a serious indicator of the danger posed by corrosion in the amine treating plants[24].

CO$_2$ induced corrosion is one of the most serious forms of corrosion in the oil and gas and transportation industry. In the presence of water, CO$_2$ forms carbonic acid which is corrosive to carbon steel [25]. Corrosion products in CO$_2$ absorption with aqueous amine solutions such as iron carbonate and iron hydroxide are insoluble and form a precipitate while the soluble products in the corrosion system include Fe(HCO$_3$)$_2$[26]. Corrosion can be explained in terms of an electrochemical reaction[23]. The overall reaction (1) involves the evolution of H$_2$ gas at the cathode (3) and reduction of Fe at the anode (2).

Overall reaction:

$$Fe + 2H^+ \longrightarrow Fe^{2+} + H_2 \tag{1}$$

Oxidation:

$$Fe \longrightarrow Fe^{2+} + 2e^- \tag{2}$$

Reduction:

$$2H^+ + 2e^- \longrightarrow H_2 \tag{3}$$
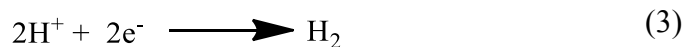
Several mechanisms have been used to postulate the corrosion phenomena observed in amine treating plants, most representing the dissolution of Fe in the CO$_2$ - water system[27]. The formation of H$^+$ can happen in many different ways as shown by (5), (6), and (8) and can be considered a driving force for metal dissolution. The greater the formation of H$^+$, greater amount of iron goes into solution to achieve equilibrium.

$$H_2O + CO_2 \rightleftharpoons H_2CO_3 \tag{4}$$

2

$$H_2CO_3 \rightleftharpoons H^+ + HCO_3^- \qquad (5)$$

$$HCO_3^- \rightleftharpoons CO_3^{2-} + H^+ \qquad (6)$$
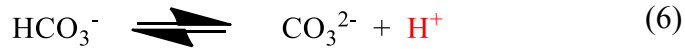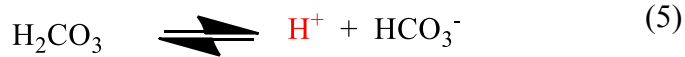
CO_2 reacts with amine to form carbamate and ammonium ion (7); the latter can dissociate to provide H^+ (8).

$$RNH_2 + CO_2 \rightleftharpoons RNH_3^+ + RNHCOO^- \qquad (7)$$

$$RNH_3^+ \rightleftharpoons RNH_2 + H^+ \qquad (8)$$
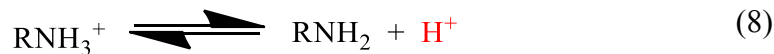
Several investigators have reported the corrosion testing on various alkanolamines - monoethanolamine (MEA), diethanolamine (DEA), methyldiethanolamine (MDEA) - in the presence of CO_2 [27-28]. Structures for these compounds are given in Table . Alkanolamines are organic bases and as such, in a pure state, are not actively corrosive towards cast iron and mild steel[29]. In the absence of CO_2, the corrosion rate of carbon steel in amine solutions were lower than those in water and that there is no difference in corrosivity among different amines. As a matter of fact, many amines are used as corrosion inhibitors[30].

From Figure , firstly, the corrosion rates of all alkanolamines are higher than 50 mpy. 1 mpy is considered an upper limit for corrosion rates to initiate control in the industry[28c]. Secondly, AMP is less corrosive than MEA while it is still higher than that of DEA and MDEA. The CO_2 loading is the key parameter in these studies. Under saturation CO_2 loading, the corrosion rates of the alkanolamines (Table) were directly proportional to the amount of CO_2 in the system. AMP has less CO_2 in the system than MEA which has higher CO_2 than DEA and MDEA under saturation conditions, and thus the trends in corrosion rates are analogous. The influence of CO_2 loading can be explained by reaction (4) - (8). Carbonic acid, ammonium and bicarbonate ions are formed at a higher rate which dissociates to form more H^+[31]. Evolution of

3

hydrogen is accompanied by more metal dissolving into solution explaining the higher corrosion rate. Under the same CO_2 loading, the corrosion rates of amines were comparable[28c]. This is attributed to the chemistry of the amine – CO_2 reaction remaining the same in all cases and the structural changes to the amine itself does not significantly affect corrosion rate.
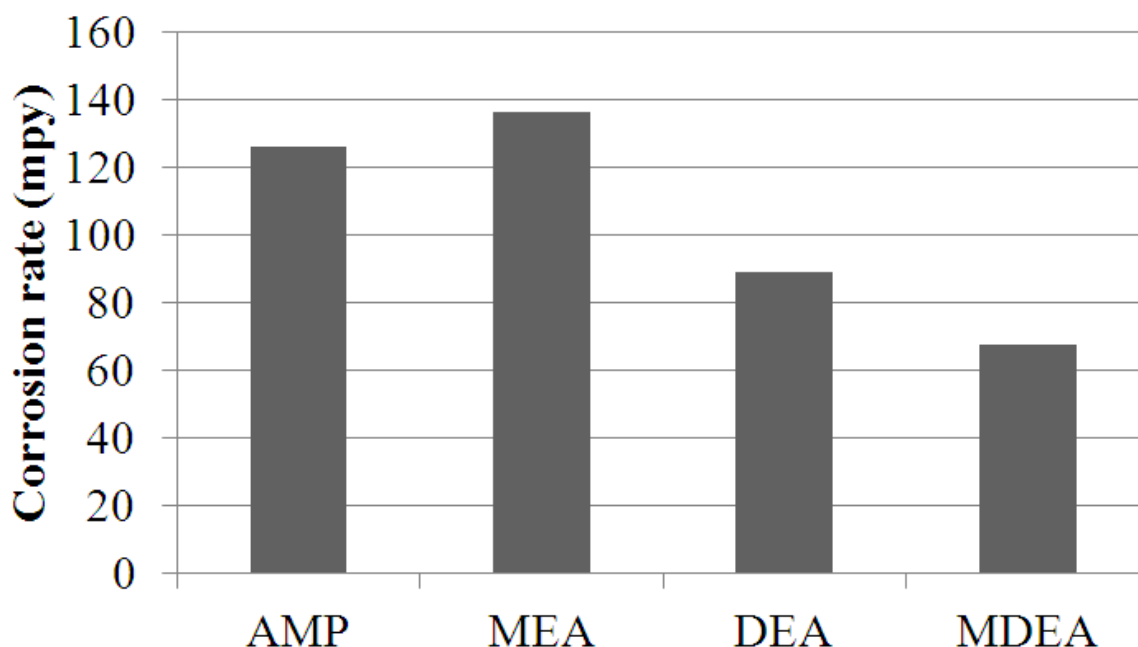
Figure : Corrosion rates of alkanolamines at 80°C, 3 kmol/m³ CO_2 saturation

There are a number of methods available for corrosion monitoring and testing. The literature discussed in this chapter uses electrochemical technique for corrosion analysis[31] which are faster and easier to perform on a lab scale. The corrosion experiments, that we performed, were using the more traditional weight loss method because the industry still uses them to monitor corrosion. Weight loss experiments required extensive manual intervention to provide information. Corrosion coupons provide a quantitative measure of coupon weight loss and a qualitative indication of the type of corrosion. Also, for this reason, the corrosion rates reported

in this study cannot be directly compared to the literature values since they were obtained by different experimental methods.

Table : Structural formulas of CO_2 absorption solvents

Type of amine	Name	CO_2 Saturation Loading (mol/mol)	Structure
Primary amine	Monoethanolamine (MEA)	0.565	HO—C(H₂)—C(H₂)—NH₂
Secondary amine	Diethanolamine (DEA)	0.442	HO—C(H₂)—CH₂ \ NH / HO—C(H₂)—CH₂
Tertiary amine	Methyldiethanolamine (MDEA)	0.243	HO—C(H₂)—CH₂ \ N—CH₃ / HO—C(H₂)—CH₂
Sterically hindered amine	2-amino-2-methyl-1-propanol (AMP)	0.554	HO—C(H₂)—C(CH₃)(CH₃)—NH₂

The motivation of this study was to investigate the corrosion of carbon steel in solutions of silylamines developed at Georgia Tech and to compare it with the industrial benchmark of monoethanolamine/water (30/70) solution. Tripropylsilylamine/water (95/5) solution was used to simulate the moisture in flue gas conditions. The excellent laboratory facilities and

knowledgeable staff at the corrosion testing group at ConocoPhillips allowed for the smooth execution of experiments.

Experimental Procedure:

Corrosion rates reported herein were obtained by weight-loss method. Carbon steel C1020 coupons (Metal samples company, Munford, AL) were used for the experiments. They were cut into rectangular shapes of dimensions of 1 in. * ½ in. * 1/16 in. with an exposed area of 1.0825 in^2 and marked with consecutive numbers. The coupons were weighed, polished and prepared in accordance with ASTM standards (ASTM G 1-03, Annual Book of STM standards ASTM International; Philadelphia 2003) before exposing them to the test solution. Fingerprints were avoided by handling the coupons with clean glove. The coupons were loaded onto the coupon holder (made of polyethylene) using Teflon strings and were lowered into the corrosion cell. The set-up consists of bench top autoclave (Figure) with temperature controllers. Aqueous solutions of the amines were prepared by batch using a digital balance with an accuracy of 0.1 g. Absorption solvents consisted of CO_2 loaded solutions of tripropylsilylamine (TPSA) and monoethanolamine (MEA). Thirty weight percent solution (remaining water) of MEA with a 30% CO_2 loading (0.3 mol CO_2/mol MEA) and ninety-five percent solution (remaining water) of TPSA with a 55% CO_2 loading (0.55 mol CO_2/mol TPSA) were prepared by purging a stream of CO_2 gas. The autoclaves were filled with the solutions and sealed with a N_2 headspace. They were heated at 100°C for duration of 30 days. The solutions were periodically checked for temperature control. Distinctive appearance of corrosion products (Figure , Figure) were seen in the case of the coupons that remained in the MEA solution. After removal, the coupons were washed with xylene to remove the oily residue on them. They were then rinsed with acetone prior to acid (solution made of 50% water, 50% HCl, 5% acid inhibitor) wash. The coupons were

6

then washed with soap and a soft brush in order to remove the corrosion products. They were then rinsed with acetone and left to dry. They were then re-weighed. Weight measurements were made with an analytical balance to the nearest 0.0001 g.

Figure : Bench top autoclave for the corrosion experiments
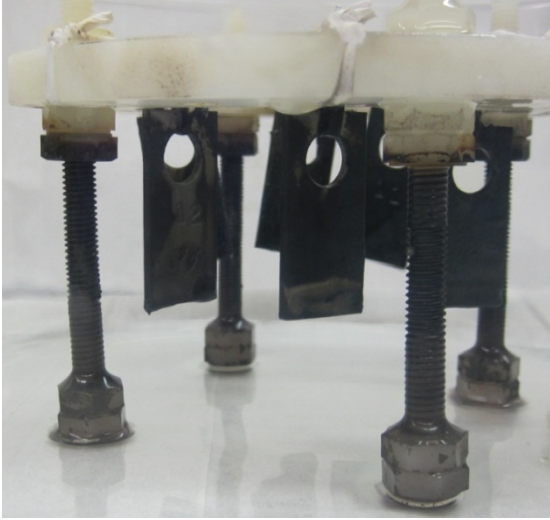
Figure : Coupons after exposure to MEA solution
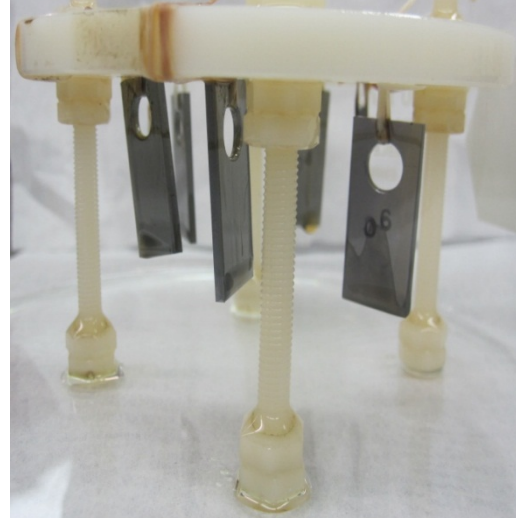
Figure : Coupons after exposure to TPSA solution

Results and Discussion:

Obtained weight loss was used to calculate the corrosion rate of the specimen using the following expression:

$$mpy = \frac{530 * W}{D * A * T}$$

Where mpy is the corrosion rate of the coupon in mils (thousandth of an inch) per year, W is the weight loss of the coupon in milligrams, D is the density of the specimen in grams per cubic centimeter, A is the area of exposure in squared inches and T is the time of exposure in hours. The corrosion rates reported in Table are the averages of values obtained from several coupons. We have also obtained values of standard deviation of the mean corrosion rate values. This standard deviation has been taken as an estimate of the uncertainty of the corrosion rate measurements and is reported for every mean value.

Figure : MEA (left) and TPSA (right) solutions after experiments

From Table , it can easily be seen that the corrosion rates of carbon steel in TPSA solution are significantly lesser than those of MEA solution. Coupons in MEA exhibited a high corrosion rate of around 10 mpy. Industrially acceptable value of corrosion rate for adequate corrosion control is 1 mpy [28a]. The corrosion rates for MEA solutions reported in the literature[28, 31] were obtained by electrochemical technique and therefore, could not be used for the comparison for the values obtained by weight loss method.

Table : Corrosion rates from weight loss experiments

Solution	Corrosion rate (mpy)	Number of coupons	% Avg. Weight loss
TPSA - water	0.05 ± 0.02	6	1.45*E-4 mg
MEA - water	9.76 ± 1.88	4	2.32*E-2 mg

The lower corrosion rate of the TPSA system is related to the surfactant effect due to the molecular structure of TPSA, thus making it a potential corrosion inhibitor. Chemistry of the TPSA system is similar to the MEA system i.e. the reactions (1) – (8) explained earlier hold valid irrespective of the amine.

Inhibition of corrosion of carbon steel can be explained on the basis of adsorption[32] and is closely related to the molecular structure. Most of the organic inhibitors contain a center like N, O, through which they are adsorbed on the metal surface. N-alkyl quaternary ammonium salts, which are similar in structure to tripropylsilylammonium, have been used extensively as inhibitors in H_2SO_4 solution[33]. The non-polar hydrocarbon chains attached to the ammonium group stabilizes the adsorbed layer in two important ways; 1) they reduce the electrostatic repulsive forces between ions of similar charges, 2) the van der waals forces of cohesion between the alkyl chains allows them to pack more closely. Previous studies have indicated this increase in inhibitor efficiency in the order of N-alkyltrimethylammonium (TMA) compounds < N-alkyltriethylammonium (TEA) compounds < N-alkyltripropylammonium (TPA) compounds consistent with the above explanation[34]. Literature also reports high inhibition efficiencies around critical micellar concentration (10^{-2} M) for a compound with a alcohol group like MEA (2-(dodecyldimethylammonio)alkanols) where the alcohol group and the long alkyl chain play a stabilizing role to the formation of the adsorbed layer[35].

There is a preliminary understanding of the mechanism by which corrosion takes place[36]. The surface of steel has induced positive (anodic sites) and negative charges (cathodic sites) derived from the simultaneous electrochemical reaction of hydrogen evolution and metal dissolution. On the cathodic sites (as depicted in Figure), adsorption of protons (H_3O^+) and desorption of hydrogen gas occur. The protonated ammonium ion (RNH_3^+) is also adsorbed electrostatically in competition. The latter is much bigger than the protons, and covers a huge portion of the iron surface resulting in the displacement of water molecules from the surface. Further, the anions in the solution – CO_3^{2-}, HCO_3^-, $RNHCOO^-$ – could then be adsorbed on the adsorbed cations resulting in closely packed inhibitor multi-layers. On the anodic sites, the

anions are first adsorbed due to chemical adsorption. Then the inhibitor molecules could be adsorbed through electrostatic attraction between the positively charged ammonium ions and negatively charged metal iron surface. These layers stack up forming a protective surface that diminishes corrosion of steel. Multilayers can be stabilized by van der waals cohesion forces among the long alkyl chains[36].
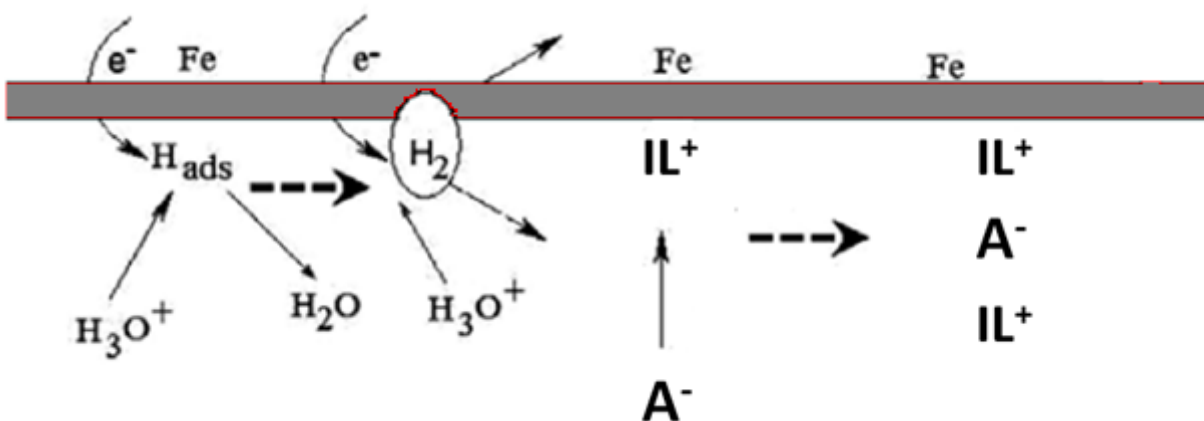

Figure : Monolayer view of possible reactions on the surface of iron

Both TPSA and MEA have reactive sites capable of adsorbing on the surface of the iron surface. TPSA has a structure which has a hydrophilic head with a long hydrophobic tail which contributes favorably to the adsorption process. The long alkyl chains allow for the formation of multi-layers on the surface of steel. We have, in fact, demonstrated the surfactant properties of TPSA by using them as reversible surfactant in the preparation of gold nanoparticles in our lab. MEA, on the other hand, has a two carbon alkyl chain which participates minimally in the stabilization of the layer although the alcohol function does play a role as described here[35]. Thus it is hypothesized that the adsorbed protective layer breaks off from the iron surface making the metal more susceptible to oxidation. This could be a possible explanation for increase in the corrosion rate with increase in temperature, where higher the temperature the adsorbed layer is more unstable.

11

Conclusions:

The development of amine systems for the removal of CO_2 from flue gas has been faced with a set of corrosion problems. The corrosion rates reported for the alkanolamine systems in literature indicate that continuous monitoring is required in the industry to ensure smooth functioning of the plant. The molecule that we propose for CO_2 capture, Tripropylsilylamine, has exhibited negligible corrosion rates making them favorable over MEA. These are attributed to the surfactant like properties of these molecules. We have a basic understanding of the mechanism by which TPSA acts like a potential corrosion inhibitor and further experiments will corroborate and extend the knowledge.

References:

1.   Ahmad, Z., *Principles of Corrosion Engineering and Corrosion Control*. 2006.

2.   Kladkaew, N.; Idem, R.; Tontiwachwuthikul, P.; Saiwan, C., Corrosion behavior of carbon steel in the Monoethanolamine - H2O - CO2 - O2 - SO2 system: Products, Reaction pathways and Kinetics. *Industrial & Engineering Chemistry Research* **2009,** *48*, 10169-10179.

3.   Barham, H.-A.; Si Ali, B.; Yusoff, R.; Kheirodin Aroua, M., Corrosion of Carbon steel in aqueous carbonated solution of MEA/[bmim] [DCA]. *International Journal of Electrochemical Science* **2011,** *6*, 181-198.

4.   Guo, X.; Y, T., The effect of corrosion product layers on the anodic and cathodic reactions of carbon steel in CO2 saturated MDEA solutions at 100C. *Corrosion Science* **1999,** *41*, 1391-1402.

5.   Veawab, A.; Aroonwilas, A., Identification of oxidising agents in aqueous amine - CO2 systems using a mechanistic corrosion model. *Corrosion Science* **2002,** *44*, 967-987.

6.   (a) Veawab, A.; Tontiwachwuthikul, P.; Bhole, S., Studies of Corrosion and Corrosion control in a CO2-AMP environment. *Industrial & Engineering Chemistry Research* **1997,** *36*, 264-269; (b) Veawab, A.; Tontiwachwuthikul, P.; Chakma, A., Influence of process parameters on corrosion behavior in a sterically hindered amine-CO2 system. *Industrial & Engineering Chemistry Research* **1999,** *38*, 310-315; (c) Veawab, A.; Tontiwachwuthikul, P.; Chakma, A., Corrosion behavior of carbon steel in the CO2 absorption process using aqueous amine solutions. *Industrial & Engineering Chemistry Research* **1999,** *38*, 3917-3924.

7.   Lang, F.; Mason, J. F., Corrosion in amine gas treating solutions. *Corrosion Science* **1958**, 105-108.

8.   Eustaquio-Rincon, R.; Rebolledo-Libreros, M. E.; Trejo, A.; Molnar, R., Corrosion in Aqueous solution of two alkanolamines with CO2 and H2S: N-Methyldiethanolamine + Diethanolamine at 393 K. *Industrial & Engineering Chemistry Research* **2008,** *47*, 4726-4735.

9.   Veawab, A.; Tontiwachwuthikul, P.; Chakma, A., Corrosion behavior in sterically-hindered amine for CO2 separation. *Greenhouse Gas Control Technologies* **1999**, 77-81.

10.   Deyab, M. A., Effect of cationic surfactant and inorganic anions on the electrochemical behavior of carbon steel in formation water. *Corrosion Science* **2007,** *49*, 2315-2328.

11.   Osman, M. M., Hexadecyl trimethyl ammonium bromide as an effective inhibitor for the corrosion of steel in sulphuric acid solution. *Anti-Corrosion methods and materials* **1998,** *45* (3), 176-180.

12.   Driver, R.; J, M. R., Inhibition by n-alkylquaternary ammonium compounds. *British Corrosion Journal* **1980,** *15* (3), 128-131.

13.   Elachouri, M.; Hajji, M. S.; Kertit, S.; Essassi, E. M.; Salem, M.; Coudert, R., Some surfactants in the series of 2-(alkyldimethylammonio) alkanol bromides as inhibitors of the corrosion of iron in acid chloride solution. *Corrosion Science* **1995,** *37* (3), 381-389.

14.   Likhonova, N.; Dominguez-Aguilar, M.; Olivares-Xometl, O.; Nava-Entzana, N.; Arce, E.; Dorantes, H., The effect of ionic liquids with imidazolium and pyridinium cations on the corrosion inhibition of mild steel in acidic environment. *Corrosion Science* **2010,** *52*, 2088-2097.

APPENDIX II

VAPOR-LIQUID EQUILIBRIUM DATA FOR THE VTMS-DODECANE SYSTEM

The fundamental understanding gained about the reactions of silane grafting of polyethylene (Chapter 1) led us to hypothesize the formation of aggregates of silanes in hydrocarbon. Vapor liquid equilibrium data has been used to study the intermolecular interactions between the solutions, and hence the deviations from ideality in the literature[11, 37]. Similar experiments were envisioned with the dodecane-VTMS system to investigate the extent of association of silanes in the hydrocarbon.

The simplistic schematic of the experimental set-up is shown in Figure . The glass vessel with a stopcock sampling valve, in which the solutions were allowed to equilibrate, was connected to a U-tube manometer and the McLeod gauge in a parallel connection using a ClearFLEX vacuum PVC tubing. The high vacuum system consisted of a vacuum pump and a cold trap. The U-tube manometer (height 12") is closed at both ends and the difference in the height of two limbs gives the absolute pressure. The readings on the scale of the manometer were read using a cathetometer. The system was allowed to equilibrate at 20°C in a constant-temperature bath (temperature control 0.01°C) with water as the heat-transfer fluid. Apiezon L grease was used inside the stopcocks and glass joints, so the system is leak-proof under vacuum. Prior to use in the experiments, the solvents were degassed using three cycles of standard freeze, pump and thaw procedure in the glass vessel. The glass vessel, along with the frozen solvent was then disconnected from the pumping apparatus and connected to the manometer and McLeod gauge system as shown below. The entire system was evacuated until the McLeod gauge reading was 0.1 mm Hg or better. The glass vessel was then allowed to equilibrate inside the constant temperature bath until manometer read a constant pressure reading. Since the scale of the U-tube

manometer was read using the cathetometer, the stability of those measurements is referred to here.

After equilibration, samples of vapor and liquid were to be removed from the system using an airtight syringe and were to be injected into a gas chromatograph. Using calibration curves for VTMS and dodecane, the concentrations of the two components in the two phases would be known. Total pressure is also known. The calculation of the activity coefficients is then straightforward from these values and with the use of Raoult's law.
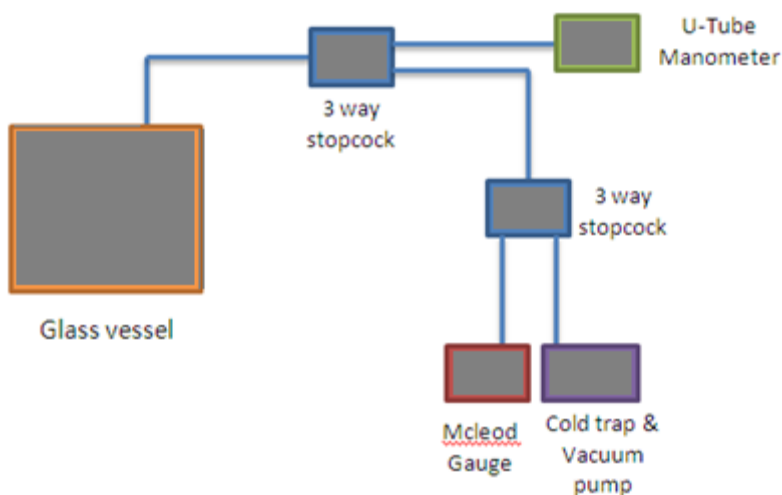

Figure : Experimental set-up for the determination of vapor pressure

Calibration curves for VTMS and dodecane were prepared by using various concentrations of VTMS and dodecane in the solvent hexane (Figure , Figure) on the GC.
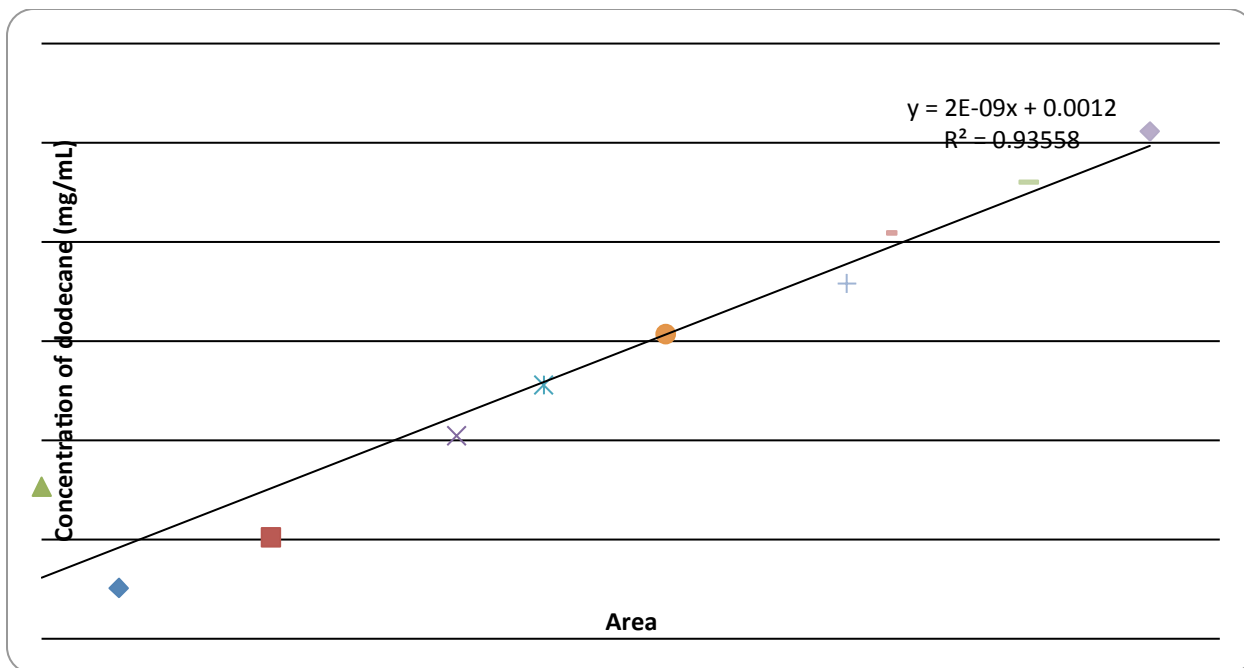
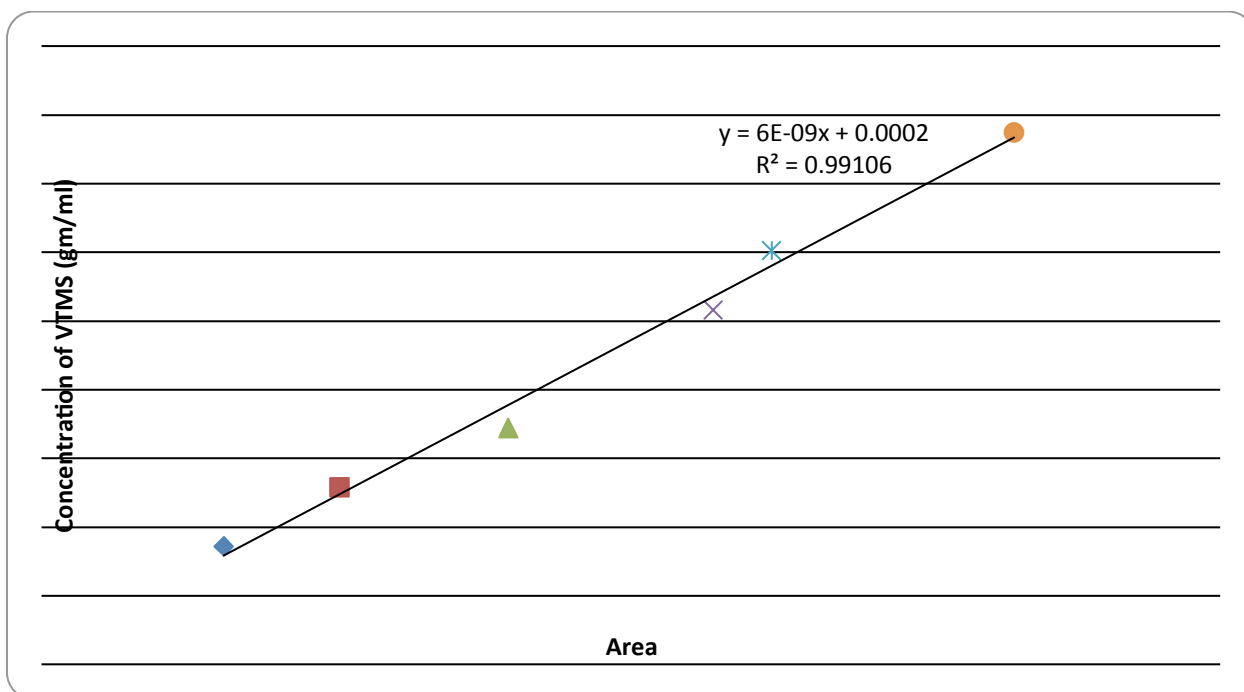**Figure : GC calibration curve for dodecane in hexane**

On the chart:
y = 2E-09x + 0.0012
R² = 0.93558

Y-axis: Concentration of dodecane (mg/mL)
X-axis: Area

Figure : GC calibration curve for VTMS in hexane

On the chart:
y = 6E-09x + 0.0002
R² = 0.99106

Y-axis: Concentration of VTMS (gm/ml)
X-axis: Area

Observations

The equilibration step of the above experimental procedure was 'never' attained during the various test runs with the solvent. It was understood that the system was not completely impervious to the surroundings and that air is being introduced into the system during the equilibration time. The pressure readings in the manometer rose constantly without staying constant, until 24 mm Hg which is the maximum the U-tube manometer is designed to measure. Prior to the above set-up, a metal canister and stainless-steel tubing was used and resulted in the same road-block for the experiment. We decided to move away from this portion of the project after significant effort.

References:

1.   (a) Eckert, C. A.; Wong, K. F., Vapor-Liquid equilibria of 1,3-butadiene systems. *Journal of chemical and engineering data* **1969,** *14* (4), 432-436; (b) Antosik, M.; Sandler, S. I., Vapor-liquid equilibria of hydrocarbons and tert-amyl methyl ether. *Journal of chemical and engineering data* **1994,** *39*, 584-587.